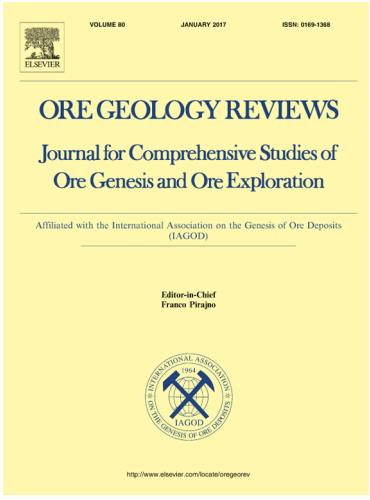

Physicochemical model for the genesis of Cu-Ag-Au-Hg solid solutions and intermetallics in the rodingites of the Zolotaya Gora gold deposit (Urals, Russia)

Valery V. Murzin, Konstantin V. Chudnenko, Galina A. Palyanova, Dmitry A. Varlamov, Evgeny A. Naumov, Franco Pirajno

PII: S0169-1368(17)30313-X
DOI: https://doi.org/10.1016/j.oregeorev.2017.12.018
Reference: OREGEO 2438

To appear in: *Ore Geology Reviews*

Received Date: 20 April 2017
Revised Date: 29 November 2017
Accepted Date: 18 December 2017

Please cite this article as: V.V. Murzin, K.V. Chudnenko, G.A. Palyanova, D.A. Varlamov, E.A. Naumov, F. Pirajno, Physicochemical model for the genesis of Cu-Ag-Au-Hg solid solutions and intermetallics in the rodingites of the Zolotaya Gora gold deposit (Urals, Russia), *Ore Geology Reviews* (2017), doi: https://doi.org/10.1016/j.oregeorev.2017.12.018

Physicochemical model for the genesis of Cu-Ag-Au-Hg solid solutions and intermetallics in the rodingites of the Zolotaya Gora gold deposit (Urals, Russia)

Valery V. Murzin[a], Konstantin V. Chudnenko[b], Galina A. Palyanova[c, d], Dmitry A. Varlamov[e], Evgeny A. Naumov [c, d], Franco Pirajno[f]

[a]*A.N. Zavaritsky Institute of Geology and Geochemistry, Ural Branch of Russian Academy of Sciences, Pochtoviy per., 7, Ekaterinburg 620075, Russia*

[b]*A.P. Vinogradov Institute of Geochemistry, Siberian Branch of Russian Academy of Sciences, Favorskogo str., 1a, Irkutsk 664033, Russia*

[c]*V.S. Sobolev Institute of Geology and Mineralogy, Siberian Branch of Russian Academy of Sciences, Akademika Koptyuga pr., 3, Novosibirsk 630090, Russia*

[d]*Novosibirsk State University, Pirogova str., 2, Novosibirsk 630090, Russia*

[e]*Institute of Experimental Mineralogy, Russian Academy of Sciences, Chernogolovka, Moscow region, 142432 Russia*

[f]*Centre for Exploration Targeting, The University of Western Australia, 35 Stirling Highway, Crawley, WA 6009, Australia*

Abstract

In this contribution we examine the compositions of solid solutions and intermetallics of the system Cu-Ag-Au-Hg and the physicochemical conditions of their formation in rodingites from the Zolotaya Gora gold deposit (Southern Urals, Russia). Thermodynamic calculations, modeling the formation of mineral assemblages of rodingite and Cu-Ag-Au-Hg mineralization, were carried out using a "Selektor-C" software package. Two probable models for the genesis of Au-Ag-Cu-Hg solid solutions and Au-Cu intermetallics in rodingites are: 1) hydrothermal; the result of single-stage discharge in open space of deep-sourced gold-bearing fluid with the composition corresponding to rodingite, taking into account its interaction with host serpentinites. 2) metasomatic; deep-seated gold-bearing fluid (W) rising to the surface interacts with early formed rodingite (R) at different ratios (W/R). T and P-conditions of modeling: 450°C, 3 kbar; 350°C, 2 kbar; 250°C, 1 kbar. Results of the calculations on the "hydrothermal" and "metasomatic" models showed different degrees of similarity of natural and theoretical model associations of rodingites. The *metasomatic model* is better for corresponding to real mineral compositions and mineral paragenesis in the natural Cu-Ag-Au-Hg system observed at

the deposit. In this model the chlorite-garnet-pyroxene rodingite is replaced by a chlorite-rich rock with increasing W/R. In this case all gold minerals of Zolotaya Gora deposit (Au-Cu intermetallics and Au-Ag solid solutions) are formed at 250-450°C. Gold-copper solid solution formed at a temperature of 450°C (W/R>10). Au-Ag-Hg solid solutions and native copper are formed only at 250°C. According to the *hydrothermal model* native copper and $AuCu_3$ were absent phases, but other Au-Cu intermetallics (AuCu, Au_3Cu) precipitate if gold concentration in the solution is higher than 0.5 ppm. Thermodynamic calculations proved the possibility of formation of equilibrium assemblages of rodingite minerals and gold-bearing minerals with the participation of water-chloride complexing and low CO_2 fluids. At a temperature < 350ºC the main status of gold in solution are $Au(HS)_2^-$ and $AuHS^0$, while at higher temperatures it occurs as $AuOH^0$. Formation of Au-Cu intermetallics occurred under the effect of weak-acid hydrothermal solutions (pH = 3.5÷5) with low fugacity of O_2 and S_2: log f_{O2} = -26 ÷ -47, log f_{S2} = -8 ÷ -20. Both models (*hydrothermal and metasomatic*) explain the formation of Au-bearing rodingites and can be used for predicting potential gold-bearing rodingite targets.

Keywords: *Zolotaya Gora gold deposit, rodingites, Cu-Ag-Au-Hg solid solutions, Au-Cu intermetallics, fluid, thermodynamic models*

1. Introduction

In this contribution, we discuss rodingites and their associated metallic mineralization. Rodingites were first recognized in the Dun Mountain ophiolite belt in New Zealand (in fact, the name derives from the Roding river near the town of Nelson, New Zealand; Williams, 1974). Rodingites are generally characterized by calc-silicate assemblages (e.g. garnet, clinopyroxene, tremolite-actinolite, and epidote) and together with albitites occur along contacts between serpentinites and country rocks (Carmichael et al., 1974; Tsikouras et al., 2009).

In most cases rodingites do not host noble metals but, occasionally they may have high concentrations of gold (Chudnenko et al., 2015; Chudnenko and Palyanova, 2016; Damdinov et al., 2004; Galuskin and Zeleg, 2003; Gunia, 1986; Kazachenko et al., 2008; Knight and Leitch, 2001; Kudryavtseva and Kudryavtsev, 2003; Murzin et al., 1987; Oen and Kieft, 1974; Rechkin,

1974; Sazonov, 1998; Zhmodik et al., 1998, 2008), silver (Leblanc and Lbouabi, 1988) or platinum (Molchanov et al., 2006). In some cases, rodingite and carbonated serpentinites may be associated with Au, Ag and Co mineralisation (Pirajno, 1992 and references therein). The Zolotaya Gora ("Golden Mountain" in Russian) gold deposit in the Karabash massif of ophiolitic ultramafic rocks in the Southern Urals, is one of these noble metals-bearing rodingites. The Zolotaya Gora deposit, in spite of its small reserves (<10 t Au), is quite unique owing to the presence of compositionally uncommon copper-bearing gold in the rocks composed of minerals usual for rodingites. This fact suggests that the rodingite of this deposit has a different origin than worldwide rodingites which usually contain no gold, and are developed as metasomatic alteration of mafic rocks.

Murzin et al. (2013) proposed a genetic model of gold-bearing rodingites in which these rocks are regarded as veins accompanied by metasomatic chloritization of the host serpentinites. In these concepts, the deposition of minerals of the system Cu-Ag-Au-Hg is coeval with the formation of rodingites, which led to the recognition of a gold-rodingite (chlogropite) type of mineral system (Berzon, 1983; Sazonov, 1998). The authors of this newly recognized type of mineral system suggest that the formation of gold-rodingite mineralization proceeded in one stage and is related to the ingress of metasomatic fluids along zones of N-S-trending tectonic dislocations. Rodingites are related to metasomatism and antigorite alteration of ultramafic rocks. Metasomatism develops simultaneously with the supply of gold-bearing fluid, approaching economic viability only in fracture zones (Sazonov, 1998).

The appropriateness of distinguishing a gold-rodingite mineralization type is doubted by some researchers. Spiridonov and Pletnev (2002) deliberate that gold is not genetically related to the formation of rodingites but is superimposed on these rocks during later carbonatization, chloritization and silicification (listvenitization; e. g. Escayola et al., 2009; Zoheir and Lehmann, 2001). Other scientists hypothesize that redistribution and concentration of gold was coeval with

the formation of bi-metasomatic rodingites, however this redistribution process was very limited (Molchanov et al., 2006; Plyusnina et al., 2007). In this case, gold is concentrated locally within the contact zones of adjacent rocks.

The key element for understanding the genesis of mineralization in rodingites from the Karabash massif is finding the answer to the question about the equilibrium of rodingite minerals with gold minerals. We made an attempt to solve this problem, using the thermodynamic modeling, which became possible by using data on the thermodynamic properties of Cu-Ag-Au-Hg solid solutions and intermetallic compounds (intermetallics). In earlier models the formation of multi-element gold-bearing solid solutions and intermetallics was commonly ignored (Akinfiev and Zotov, 2010; Pokrovski et al., 2014).

Experimental and numeric modeling of the process of rodingitization for the system Mg–Ca–Fe–Si–Al–Na–Cl–O–H was conducted by Plyusnina et al. (1993) and Bach and Klein (2009). However, the model system in these works lacked such elements as Au, Ag, Cu, Hg and the role of solid solutions and intermetallics was not considered. Palandri and Reed (2004) carried out calculations in the temperature interval 25-300°C and used an ideal model for solid solutions. Recently, thermodynamic properties of solid phases of six binary subsystems (Ag-Au, Au-Cu, Ag-Cu, Ag-Hg, Au-Hg, Cu-Hg), two ternary subsystems (Cu-Ag-Au, Ag-Au-Hg) and one quaternary system Cu-Ag-Au-Hg have been estimated (Chudnenko and Pal'yanova, 2013a,b, 2014, 2016; Liu et al., 2012; Pal'yanova, 2008).

This paper is aimed at the thermodynamic modeling of the formation conditions of rodingite mineral paragenesis, including the presence of binary, ternary and quaternary solid solutions and intermetallics in the system Cu-Ag-Au-Hg, to solve problems of the genesis of the Zolotaya Gora gold deposit and other similar occurrences.

2. Geology of the Karabash massif and the Zolotaya Gora deposit

The Karabash massif of ophiolite ultramafic rocks occurs in Southern Urals, about 100 km west of Chelyabinsk city. It extends approximately in a N-S direction and is localized in the zone of the Main Ural fault which separates the paleo-continental and paleo-oceanic sectors of the Urals. At the latitude of Karabash town this zone is made up of serpentinized ultramafic rocks within Ordovician oceanic and island-arc sedimentary-volcanic complexes of the Silurian-Devonian Tagil-Magnitogorsk terrain (Fig. 1) described in Russian publications as "megazone" (Puchkov, 2010, 2017). From east to west, the massif, which is 15 km long, borders on volcano-sedimentary, predominantly marmorized limestones, basalt and andesite-basalt.

The Sm-Nd age of formation of rodingites is 369.4±8.8 Ma (Murzin et al., 2013), which coincides with the period of early collision and compression of Ordovician oceanic and Silurian-Devonian island-arc complexes and upward movement of the block of ultramafic rocks (Seravkin et al., 2003; Puchkov, 2017), including the Karabash massif.

The Karabash massif is composed of antigorite, and to a lesser degree, chrysolite and lizardite serpentinites. The massif also contains isolated bodies of rodingites, magnetite-chlorite-carbonate, quartz-riebeckite rocks and listvenites. All these lithologies have a similar geologic setting, being localized in the zones of tectonic mélange; listvenites are found only in the southwestern contact of the massif (Murzin et al., 2013) (Fig. 1).

The belt of rodingites can be traced for about 2.5 km along the central part of the massif. Some bodies of rodingites extend for about 600–700 m and are composed of aggregates of three main minerals: diopside, garnet and chlorite in varying quantities. Rodingite has tectonic contacts with the hosting serpentinites (Fig. 2a). In the endocontact of rodingite serpentinites are strongly chloritized and can be called "chloritites". Massive rodingites and chloritites exhibit a network of cross-cutting veinlets of diopside and calcite. Veinlets of diopside often penetrate from the rodingite into the host rocks (Fig. 2b).

Throughout the whole belt, rodingites are gold-bearing, but the gold-richest are in its central part, namely the Zolotaya Gora deposit, abandoned at a depth of 200 m. Both the vein-like rodingite and the fragments of chloritite occur within the ore bodies. The ore bodies are steeply dipping 60–70° southeastward. The average thickness of ore bodies is about 2–3 m, varying from 0.1–0.3 m to 8 m. Below 200 m, mineralization does not wedge out, but the gold content, reaching a few hundreds ppm in the upper horizons and averaging 5-6 ppm, drops substantially.

Typically, even in the ores with a high gold content the amount of ore minerals is very low. Only magnetite, ilmenite and chalcocite may occur in amounts of up to 2–3 wt.%. The average content of sulfides in the ores is no more than 1 wt.%, and the total content of sulfur is 0.2 wt.%.

3. Mineralogy, stages and conditions of formation of rodingites from the Karabash massif

The mineral composition of rodingites from the Karabash massif was studied by many researchers (Berzon, 1983; Lozhechkin, 1935, Novgorodova et al., 1977; Perelyaev, 1948; Pokrovsky et al., 1979). The most complete data on the composition of minerals and sequence of their deposition were obtained by Spiridinov and Pletnev (2002) who proposed a two-phase formation of gold-bearing rodingites.

Based on the earlier data (Murzin et al., 2013; Spiridinov and Pletnev, 2002) we propose a 3-stages formation of gold-bearing rodingites (Table 1). First stage rodingites are fine- and medium-grained chlorite–garnet (andradite)–diopside rocks with various ratios of these constituent minerals. Synchronously with them, host serpentinites are altered into a rock made up almost completely of fine- and small-grained chlorite with relict serpentine. The second stage is spread among early rodingites as non-uniformly distributed 0.1 m thick sheeted veinlets

158 composed of coarse-grained diopside with lesser amounts of chlorite, hydroandradite, magnetite
159 and ilmenite. In places, diopside veinlets go beyond the rodingite bodies into host chloritite rocks
160 and serpentinites. These rocks are repeatedly chloritized through a network of thin joints to form
161 coarser-grained aggregates. In the third stage formation of rodingites was completed by the
162 deposition of small amounts of calcite. In rodingites, calcite occurs as thin veins and small nests
163 (2-3 cm). In some cases, it replaces the earlier deposited Ti-andradite and, to a lesser degree,
164 diopside to form a small amount of quartz, magnetite and titanite. Small sites of calcite-chlorite
165 rocks are also present in chloritites and serpentinites.

166 All stages are gold-bearing. Gold particles in rodingites fill cleavage cracks in diopside,
167 cement the laminated mass of chlorite, and form intergrowths in garnet and magnetite. In calcite
168 veinlets we found rare micro-inclusions of native gold without traces of other elements, except
169 silver. Spiridonov and Pletnev (2002) detected also the presence of Cu in native gold.

170 At the Zolotaya Gora deposit, rodingites of the first and second stages formed under the
171 conditions typical of rodingites: T = 420–470°C, P = 2–3 kbar, X_{CO2} = 0.001–0.02 (Murzin and
172 Shanina, 2007; Murzin et al., 2013). The third and final stage proceeded with a decrease in P-T
173 (0.5–1 kbar, 230–310°C) and an increase in X_{CO2} to 0.04. The gas composition of the
174 rodingitizing fluid is represented by the C–H–O system with a minor content of nitrogen (X_{N2}
175 less than 0.002) and lack of H_2S. The fluid is characterized by an extremely high mole fraction of
176 water (X_{H2O} = 0.942–0.981), with a predominance of hydrogen among gas components (X_{H2} =
177 0.012–0.023), substantially chloride-magnesium salt composition, with a small amount of
178 chlorides of calcium and iron, and low salinity (2.6–6.7 wt.% NaCl eq.). Rodingites of the first
179 and second stages formed under reducing conditions (ratio of volatile components
180 $CO_2/(CO_2+CO+H_2+CH_4)<0.35$), and the calcite veinlets of the third stage formed under
181 oxidizing conditions ($CO_2/(CO_2+CO+H_2+CH_4)=0.83$). The oxidation level of the fluid on

serpentinization is characterized by intermediate values $CO_2/(CO_2+CO+H_2+CH_4)$=0.41-0.52 (Murzin and Shanina, 2007).

4. Chemical composition of Cu-Ag-Au-Hg solid solutions and Au-Cu intermetallics from the Zolotaya Gora deposit

Mineralogy and petrography of the rocks was studied using an Olympus BX-51 optical microscope. The chemical composition of native gold, borrowed from Pokrovsky et al., (1979), was determined by X-ray spectral microanalysis (JXA-5a). In this study scanning electron microscope CamScan MV2300 (VEGA TS 5130MM) equipped with an energy dispersive X-ray spectrometer INCA Energy 350 was used. The photomicrographs were taken using a high-contrast BSE shooting mode with an increased absorption current on the sample and an extended exposure time (up to 10 minutes), which allows the separation of phases with a difference of less than 1 atomic number. Studying of thin mineral aggregates was made to determine the primary composition of the decomposed solid solution. Study performed with multiple scanning mode for the chosen area 18x18 or 36x36 μm with the resolution 1024x1024 pixels or higher (minimal scanning time was 180 seconds) with accumulation of cooperative EDS spectrum. It allows to make rather correct averaging of composition of the studied area.

Native gold from the Zolotaya Gora deposit has a very specific chemical and phase composition as well as structure of its particles. It was shown in the earliest works that gold has non-uniform phases and occurs as lamellar intergrowths of Au-Cu alloys and electrum formed as exsolution products of solid solution (Lozhechkin, 1935; Perelyaev, 1948). Later, gold-copper minerals phases were defined with composition close to AuCu (tetra-auricupride, rozhkovite, cuproauride), $AuCu_3$ (auricupride) and Au_3Cu, and among gold-silver minerals, a wide range of phases from high-fineness gold to native silver, containing up to 12 wt.% Hg (Novgorodova et

al., 1977; Pokrovsky et al., 1979; Spiridonov and Pletnev, 2002). Moreover, native copper and mercury-bearing silver were also found at the deposit (Spiridonov and Pletnev, 2002).

Compositions of gold minerals are presented in the diagram shown in Fig. 3. The gold minerals in the ores from the Zolotaya Gora deposit reported by Spiridonov and Pletnev (2002) is as follows: 45% AuCu (tetra-auricupride), 25% auricupride ($AuCu_3$), 15% exsolution products of Au-Cu solid solutions, 5% Au_3Cu phase, 10% Au-Ag amalgams and only 1% native gold and silver. The chemical composition of some minerals is close to the stoichiometric ratios of components with only minor deviations. Wide variations are typical of the Au_3Cu phase: $Au_{2.70-2.96}Ag_{0.03-0.07}Cu_{0.99-1.24}$ (also contains to 0.6 wt.% Hg) (Spiridonov and Pletnev, 2002). Silver content in gold-copper minerals generally does not exceed 3 wt. % according to microprobe analysis or 10 wt.%, data of bulk chemical analysis (Pokrovsky et al., 1979). Native copper contains impurity of silver (to 0.18 wt. %) and gold (to 0.56 wt. %) (Spiridonov and Pletnev, 2002).

Detailed XRD studies of the Au-Cu alloys and mercurian gold showed that they are represented by the products of solid-phase modification of relatively high-temperature solid solutions of the system Cu-Ag-Au-Hg (Murzin and Sustavov, 1989; Novgorodova et al., 1977; Pokrovsky et al., 1979). As the temperature decreases owing to the drastic restriction of the stability of solid solutions, they experience a multistage decomposition into lamellar and latticed aggregates of Au-Ag-Hg and Au-Cu phases. The exsolution was accompanied by the phenomenon of ordering of the structure of Au-Cu phases and formation of intermetallics. Ordering of the structure takes place in synthetic alloys at 390-410°C by way of nucleation and growth of the ordered phases precipitated from solid solutions (Vol and Kagan, 1976). The maximum degree of ordering is achieved in solid solutions that are close in stoichiometry of $AuCu_3$ and AuCu. As a result of solid-phase transformations, the phase composition of gold particles becomes more complicated and their present-day microstructure becomes extremely

non-uniform (Fig. 4). We believe that the main volume of gold in the deposit formed during the earlier first and second stages and is composed of exsolved Au-Ag-Cu solid solutions with a wide range of compositions from Au_3Cu to $AuCu_3$ as well as associated Au-Ag-Hg solid solutions and ordered phases AuCu (tetra-auricupride) and $AuCu_3$ (auricupride).

The specific features of the structure and composition of gold minerals are shown in Figs. 3 and 4. The most common is Au-Cu-Ag-Hg solid solution, the initial composition of which was calculated by averaging EMP results obtained in the raster scan of grain fragments and equals to (in wt.%): Au 80.2-83.6; Ag 0.5-0.9; Cu 17.9-19.6; Hg 0.1-0.3 or $Au_3Cu_2Ag_{0.0n}Hg_{0.0n}$. The exsolution products of this solid solution consist of alternating thin plates of tetra-auricupride (in wt.%: Au 76.2-78.2; Ag 0.1-0.3; Cu 20.0-20.2) and Au-Cu solid solution with trace contents of silver and mercury (in wt.%: Au 83.8-85.0; Cu 10.9-11.1; Ag 1.1-1.6; Hg 0.0-1.3 or $Au_2CuAg_{0.0n}Hg_{0.0n}$) (Fig. 4a). The plates of Au-Cu solid solution contain inclusions of Hg-bearing high-fineness gold (in wt.%: Au 88.0; Ag 12.0; Cu-0.1; Hg 0.9) (Fig. 4b) formed, probably, during further exsolution of this solid solution.

Less frequent is the Au-Cu solid solution, variations of the chemical composition of which range from $AuCu_3$ to $AuCu_2$. Its exsolution product is a fine mixture of auricupride $AuCu_3$ and Au_3Cu phase (Murzin and Sustavov, 1989).

Auricupride and tetra-auricupride of stoichiometric compositions make up particles in the chlorite-garnet-pyroxene rock and veinlets of diopside. They are intergrown with mercury-bearing electrum (Fig. 4c,d). Garnet-pyroxene rodingite also contains particles composed of tetra-auricupride in the core and auricupride in the rims. It was established that the inclusions of mercury-bearing electrum in auricupride are concentrically zoned from center to periphery, and a simultaneous increase in the contents of silver (from 45 to 56 wt.%) and mercury (from 1-2 to 12 wt.%) was also observed (Pokrovsky et al., 1979).

Phase Au_3Cu is described in Spiridonov and Pletnev (2002) as overgrowths and substitution rims on auricupride and tetra-auricupride. Most likely, this phase formed during the third stage. This stage also involved deposition of mercury-free Au-Ag solid solution as well as native silver and copper.

Native copper in the Karabash massif occurs in antigorite serpentinites developed after harzburgite. In rodingites, native gold containing up to 0.5 wt.% mercury was described as xenomorphic particles or inclusions in auricupride (Spiridonov and Pletnev, 2002). We have found grains of native copper up to 1 mm in size in calcite veins. They are replaced by cuprite along the margins.

5. Methods used and initial data for thermodynamic modeling

5.1. Software used and thermodynamic dataset

We used the software "Selektor-C" (Chudnenko, 2010) for the modeling of physicochemical processes of the formation of Cu-Ag-Au-Hg mineralization in rodingites. This software is implemented in the application of the method of thermodynamic modeling on the basis of the approach of convex programming (Karpov et al., 1997). Earlier we used the "Selektor-C" software to study the formation of mercurian gold at Kyuchyus Au-Sb-Hg deposit (Chudnenko et al., 2015) and the quaternary solid solutions under hydrothermal conditions at the Aitik Au-Ag-Cu porphyry deposit and the formation of Au-Cu solid solutions and intermetallics at the Wheaton Creek placer deposit (Chudnenko and Palyanova, 2016).

The calculation of relationships for aqueous solution components was performed using the modified equation HKF (Tanger and Helgeson, 1988). The dependence of thermodynamic characteristics of gases on pressure was calculated from modified Benedict–Webb–Rubin state equation (Lee and Kesler, 1975). In the high pressure zone, a deviation from ideal gas mixture

for real gases is calculated using the Van der Waals equation (Walas, 1985) and (Breedveld and Prausnitz, 1973). Fugacity coefficients and mole gas volumes were calculated using the two- (Breedveld and Prausnitz, 1973) and three-parameter (Lee and Kesler, 1975) equations of state.

Modeling was carried out for the system Na–K–Mg–Ca–Al–Si–Ti–Mn–Fe–Cu–Ag–Au–Hg–S–Cl–C–H–O. Thermodynamic properties of various compounds were calculated using the Selektor-C databases. The list of the minerals, aqueous and gaseous species in the corrected model is presented in Tables 2 and 3. Experimental studies of the formation of the Au-Ag-Cu alloys using differential scanning calorimetry (DSC) (Amiour et al., 2014) have shown that the $AuCu_3$ and AuCu phases can stay stable up to 500°C, so in our models the range of temperature boundaries of these minerals was broadened. Chlorites, garnets, pyroxenes, carbonates, olivine, plagoiclase, K-feldspar and Cu-Ag-Au-Hg solid solutions, activity coefficients of end-members are calculated according to the conventional models of solid solutions (Chudnenko, 2010; Chudnenko and Palyanova, 2016).

5.2. Initial data for thermodynamic modeling

In order to make a model with "Selektor-C" software (Chudnenko, 2010), calculations on mineral equilibrium of rock-forming minerals of rodingites and minerals of the system Cu-Ag-Au-Hg were conducted. Two probable models of formation of Cu-Ag-Au-Hg solid solutions and Au-Cu intermetallics in rodingites are: 1) hydrothermal; the result of single-stage discharge in open space of deep-sourced gold-bearing fluid with the ratios of components corresponding to rodingite, taking into account its interaction with host serpentinites. 2) metasomatic; deep-seated gold-bearing fluid (W) rising to the surface interacts with rodingite (R) at different ratios (W/R). T-P conditions of modeling: 450°C, 3 kbar; 350°C, 2 kbar; 250°C, 1 kbar. According to the data of fluid inclusion study (gas chromatography) for both models we took a weak-

303 acid−CO_2−water−chloride (0.4 mol.% CO_2, 0.2 mol.% HCl and 1.4 mol.% H_2 in 1 kg water)
304 solution (Murzin and Shanina, 2007).

305 In the hydrothermal model, the discharging fluid with the content of other components
306 equivalent to the composition of conventional rock consisting of 100 g rodingite and 1 g
307 serpentinite. The chemical composition of typical chlorite-garnet-pyroxene rodingite and
308 serpentinite used for calculations is given in Table 4. The content of S in rodingite (0.07 wt.%)
309 corresponds to its minimal values in the available analyses. The contents of Ag (2.22 ppm), Hg
310 (0.56 ppm) and Cu (760 ppm) in rodingite were estimated using the data of ICP-MS analysis
311 (Institute geology and Geochemistry of the Urals Branch of the Russian Academy of Sciences).
312 As gold content in ores varies strongly, we calculated the variants of the model for different
313 amounts of Au in the fluid from 0.1 to 10 ppm.

314 In the metasomatic model, the initial rock, represented by 100 g rodingite and 1 g
315 serpentinite, interacts with weak-acid−CO_2−water−chloride solution. The initial composition of
316 fluid is calculated for the conditions of thermodynamic equilibria in the supercritical region at
317 650°C and 4 kbar (Table 5) based on the ratio of components 0.4 mol.% CO_2, 0.2 mol.% HCl
318 and 1.4 mol.% H_2, dissolved in 1 kg water (Murzin and Shanina, 2007). The quantity of Hg,
319 owing to limited data, is taken according to average mercury contents in hydrothermal fluids in
320 gold deposits (Chudnenko et al., 2015). It is worth noting that the increased ore contents of high-
321 temperature H_2O-CO_2 fluid with respect to gold and silver have been discussed for a long time
322 (Kolonin et al., 1994, 1997; Laptev and Pal'yanova, 2001; Normand and Williams-Jones, 2007;
323 Pokrovski et al., 2014). The potential capacity of these solutions for copper and mercury is here
324 estimated for the first time. The hydrothermal and metasomatic models are discussed in more
325 detail in the sections below.
326

6. Results of thermodynamic modeling

6.1. Hydrothermal genetic model of gold-bearing rodingites

Forms of transfer of Au, Ag and Cu in the initial model hydrothermal solution (containing 1 ppm Au) are shown in Fig. 5. The sulfide complexes of gold $Au(HS)_2^-$ and $AuHS^0$ are predominant up to 350ºC, whereas at higher temperatures (>400ºC) the main status of gold in hydrothermal solution is $AuOH^0$ (Fig. 5a). In solid phases below 350ºC there is an Au-Ag solid solution with minor admixtures of copper and mercury. At 400ºC, AuCu intermetallic compound is formed, then with increasing temperature the Au-Cu-Ag-Hg solid solutions appeared again. (Fig. 5b). Silver and copper in hydrothermal solution are represented both by sulfide and chloride complexes. Sulfide complexes of silver and copper prevail at lower temperatures, but starting from 350ºC, the importance of chloride and hydroxide complexes increases (Fig. 5c,e). In solid phases, Ag is contained in Au-Ag-Cu-Hg (Fig. 5d) solid solution only; Cu is contained mainly in sulfides, such as chalcopyrite (T<300ºC), bornite (T<450º) and chalcocite (T>350ºC), and rarely in Au-Ag-Cu-Hg (Fig. 5f) solid solution. Mercury in the hydrothermal solution occurs as Hg^0, with chloride and sulfide complexes of mercury being present in minor amounts.

In the hydrothermal model the formation of rodingite including gold-silver associations may result from a single discharge of hydrothermal solutions. The mineral composition obtained as a result of thermodynamic modeling corresponds to the paragenesis of three main rock-forming minerals observed in the deposit - chlorite, garnet and pyroxene - in the following ratios (wt.%): 36:20:44 (T=450°C), 37:17:45 (T=350°C) and 38:9:49 (T=250°C), respectively. As the temperature decreases, the amount of carbonates increases to 4 wt.% (T=250°C).

The paragenesis of gold minerals depends on the T-P conditions and the specified initial amount of gold in the fluid. At T = 450°C, the fluid with log f_{S2} = -8.3 and log f_{O2} = -27 is the source for the formation of AuCu intermetallic, which starts to quantitatively exceed the phase of

disordered solid solution Au-Ag-Cu-Hg if the content of Au in the fluid is > 0.8 ppm (Fig. 6a). The disordered solid solution Au-Ag-Cu-Hg at T = 450°C is represented by a copper-bearing Au-Ag alloy with the ratios of components from $Au_{0.3}Ag_{0.7}$ to $Au_{0.4}Ag_{0.6}$ (Fig. 6b).

A decrease in fluid temperature to 350°C leads to a change in redox conditions (log f_{S2} = -9.7 and log f_{O2} = -32) and to formation of the disordered solid solution Au-Ag-Cu over the entire Au content range of 0.1-10 ppm (Fig. 6c). The disordered solid solution Au-Ag-Cu here consists of a copper-bearing Au-Ag alloy with the ratios of components from $Au_{0.2}Ag_{0.8}$ if the content of Au in the fluid is 0.1 ppm to silver-bearing Au-Cu alloy $Au_{0.74}Cu_{0.24}Ag_{0.03}$ if the content of Au in the fluid is 10 ppm (Fig. 6d).

A decrease in temperature to 250°C results in further reduction of oxidation potentials (log f_{S2} = -12.6 and log f_{O2} = -40), forming intermetallic Au_3Cu, which predominate over the solid solution Au-Ag-Cu-Hg when Au content in fluid is higher than 6 ppm (Fig. 6e). The Au-Ag solid solution has the composition from $Au_{0.2}Ag_{0.8}$ to $Au_{0.9}Ag_{0.1}$ with impurity of mercury to 1 mol. % (Fig. 6f).

6.2. Metasomatic model for the formation of gold-bearing rodingites

The metasomatic model involves various stages of fluid interaction with rocks when the initially acidic solution at first became close-to-neutral, then weakly alkaline and later, alkaline. The initial chlorite-garnet-pyroxene composition of rodingite is stable in the temperature range of 250-450°C, under the conditions of rock-dominant regime (W/R < 1). In fluid-dominant conditions (1 < W/R < 30), rodingite composition tends to a pyroxene-chlorite assemblage (Fig. 7a,c,e). An increase in W/R > 30 the fraction of chlorite increases leading to the formation of chloritite. The latter is accompanied by a small amount of other minerals: talc and tremolite at 350-450°C, carbonate, talc, tremolite and quartz at 250°C. The calculated model also contains accessory minerals (less than 1 wt.%), mainly sulfides of copper and iron. At 450°C, 3 kbar

redox conditions correspond to a change of troilite by bornite-chalcocite buffer and log f_{S2}, from -5.7 to -9.5 (Fig. 7b). At 350°C, 2 kbar the change in f_{S2} is similar to the previous case, when the second buffer is represented by bornite-chalcocite-chalcopyrite composition, with increase in the total amount of iron and copper sulfides log f_{S2} from -8 to -15.8 (Fig. 7d). If T-P is reduced to 250°C and 1 kbar, the obtained features do not basically change, except for the addition of pyrite to the composition of the second buffer and with precipitation of native copper (W/R>50), log f_{S2} from -12 to -20 (Fig. 7f). When log f_{O2} goes to a stable level, the fugacity of S_2 decreases with increasing W/R for given T and P at W/R> 0.7 (T= 450°C), W/R > 1 (T= 350°C), W/R > 5 (T= 250°C).

Intermetallics and solid solutions of gold with copper, silver and mercury, formed in the metasomatic model are shown in Fig. 8. The formation of AuCu and $AuCu_3$ was observed during the interaction of rodingite with fluids over the whole range of 250-450°C. AuCu predominates at 350-450°C, where this mineral exists in a wide range of W/R ratios. At 250°C it is formed only with W/R ~ 100. On the contrary, auricupride ($AuCu_3$), begins to predominate with temperature decrease and usually form at the initial stages of water/rocks interaction (W/R <= 0.1). Formation of Au_3Cu mineral was found at the interaction of fluid with T = 250°C and high W/R >10. The calculations indicate that gold concentration in the ores can reach more than 10 ppm (see Fig. 8a).

The solid solutions of the system Au-Ag-Cu-Hg are present across the whole range of temperatures. The amount of gold in them increases toward an increase of the W/R ratio. These solutions are the main gold carriers in ore which formed under rock-dominant conditions (0.1 < W/R < 10). An increase in W/R > 10 or decrease W/R < 0.1 makes their amount comparable to Au-Cu intermetallics.

Gold-silver solid solutions with a minor admixture of Cu, or gold-copper solid solutions with an admixture of Ag are formed (Fig. 8b,d,f). In composition of Au-Ag solid solutions, at

W/R <10 gold prevails over silver (Au:Ag = 6:1 - 8:1) , but at W/R> 10 and T = 350-450°C, on the contrary, silver can prevail over gold (Au:Ag = 3:6 - 4:5). The solid solution Au-Cu (Au:Cu ~ 2:3) with minor amounts of Ag forms at the low W/R ~ 0.1 (Fig. 8b,d,f) and at the high W/R~100, T = 450°C (Fig. 8b). It is interesting that the formation of gold-silver amalgams Au-Ag-Hg and native copper takes place only when rodingite interacts with a low-temperature fluid (250°C).

Modeling at different P-T conditions and W/R ratios (Figs.7, 8) allows estimation of the influence of redox conditions on the formation of gold-bearing minerals. The formation of solid solution Au-Ag-Cu-Hg is probable in a wide range of W/R at log f_{S2} from -5.5 to -9.5 (450°C), from -8 to -16 (350°C), from -12 to -20.4 (250°C); log f_{O2} from -26.5 to -30 (450°C), -32 to -38 (350°C), -39 to -47 (250°C); pH = 4.5 – 9.8. The field of formation of Au-Cu intermetallics is log f_{S2} from -6.5 to -20.4; log f_{O2} from -26.5 to -47; pH = 4.5 – 9.8 (Table 6).

7. Discussion

7.1. Rodingite mineral assemblages and physical-chemical conditions of its formation

According to present-day concepts, rodingites, which are common in ultramafic rocks, are the products of “diffusive” bi-metasomatism (Coleman, 1977; Likhoidov and Plyusnina, 1992; Plyusnina et al., 1993; Palandri and Reed, 2004). They locally occur along the contacts of ultramafic rocks with rocks of contrasting composition. Rodingites contain both high-temperature minerals – pyroxene, garnet, wollastonite and vesuvian, and lower-temperature minerals – zoisite, epidote, clinozoisite, chlorite, calcite, xonotlite, prehnite, albite, etc. Mineral assemblages of rodingites are formed at temperatures ranging from 500 to 250°C and pressures of 4.5 to 1 kbar (Dubincka et al., 2004; Koutsovitis et al., 2013; Mittwede and Schandl, 1992; Normand and Williams-Jones, 2007; Plyusnina et al., 1993; Schandl and Mittwede, 2001; Schandl et al., 1990).

Analyses of gas-liquid inclusions in rodingite minerals were performed by Schandl et al. (1990), Mittwede and Schandl (1992), O'Hanley et al. (1992), Vallis and Scambelluri (1996), Schandl and Mittwede (2001), Knight and Leitch (2001), Spiridonov and Pletnev (2002) and Dubincka et al. (2004). According to published results a typical feature of rodingitizing fluid is its low salinity (less than 10 wt.% NaCl eq.). Homogenization temperatures of inclusions from garnet, diopside, clinozoisite and calcite are in the range of 190-330°C.

Experimental and thermodynamic modeling of rodingites shows that the main factors governing the mineral composition of rodingites are temperature and composition of fluid phase, especially the amount of carbon-dioxide (Likhoidov and Plyusnina, 1992; Plyusnina et al., 1993; Koutsovitis et al., 2013). According to the data of these authors, the optimum conditions for the formation of the vesuvianite-garnet-pyroxene rodingites are: temperatures 450-350°C, P = 2-4 kbar and a low concentrations of carbon-dioxide - $X_{CO2} < 0.02$. At lower temperatures and increased X_{CO2} up to 0.1, diopside, garnet and vesuvianite are replaced by tremolite, chlorite, calcite, quartz, pectolite.

We also estimated the effect of the CO_2 content in the fluid for the composition of the mineral assemblages formed according to the metasomatic model. The initial composition of the fluid was chosen taking into account different degrees of its saturation with CO_2: 0.4, 4.0 and 40 mol. % of CO_2. Calculations for the T = 250-450°C show that when the CO_2 content in the fluid is above 0.4 mol.% in composition of the resulting rock sharply increases amount of carbonate, quartz, and at high W/R also graphite (Fig. 9). These data convince us in the correct choice of the low carbon dioxide content in the fluid ($X_{CO2} = 0.004$), chosen for model calculations, since the amount of carbonate in rodingites of the Karabash massif is very low (less than 1-2 vol.%), and there is no quartz and/or graphite.

7.2. Results of thermodynamic modeling and implications of rodingites from the Karabash massif

Fig. 10 shows the associations of rock-forming minerals of rodingites and ore minerals, including Au-Cu intermetallics and Au-Ag-Cu-Hg solid solutions, obtained from hydrothermal and metasomatic models. Below we present a comparative analysis of calculated model and natural mineral associations.

Hydrothermal model of formation of gold-bearing rodingites. The obtained data on the mineral composition of rodingites formed on the discharge of low-CO_2 fluid at different temperatures, agree with the observed contents of these rocks in the Zolotaya Gora deposit. The groundmass of rodingites of the first and second stages in this deposit formed by the discharge of the high-temperature fluid (400-500°C), and the rodingites themselves are composed of chlorite, pyroxene and garnet. The accessory ore minerals in these rodingites, chalcocite, bornite and chalcopyrite (see Table 1) are also reported in the results of calculation on the hydrothermal model. The appearance of carbonate in the model calculations is related to the discharging of fluid with lower P-T parameters, reflecting the thermobaric stability conditions of minerals of stage 3 (chlorite, calcite, magnetite) at T < 300°C. The amount of carbonates in rodingites from the Zolotaya Gora deposit is small, which can be due to the low content of CO_2 in the rodingitizing fluid.

The calculations performed also revealed mineral phases of gold, which are in equilibrium relation with rodingite minerals. These are Cu-bearing Au-Ag and Ag-bearing Au-Cu solid solutions as well as intermetallics of AuCu and Au_3Cu. All these phases were established in the composition of mineral paragenesis of rodingites from the Zolotaya Gora deposit (see Table 1). Same time native copper and $AuCu_3$ were absent among of mineral phases.

The temperature ranges of the formation of rodingites of the first and second stages from the Zolotaya Gora deposit (420-470°C) agrees with the modeled deposition conditions of Au-Ag

solid solutions and tetra-auricupride, as a result of fluid discharge with a T = 450ºC. Au_3Cu in the deposit occurs rarely and in small quantities. This mineral forms in the stage 3 of rodingites formation. The temperature range of the third stage minerals (310-230°C) conforms to both the stability conditions of Au_3Cu in the hydrothermal model under 250°C (see Fig. 6e) and the critical temperature of ordering of solid solution of this composition at 230°C (Vol and Kagan, 1976).

The Ag-bearing Au-Cu solid solution was obtained in calculations under the high gold content in the fluid (> 2 ppm) at 350°C (see Fig. 6d). The chemical composition of this solid solution is close to the fine mixture phases at the Zolotaya Gora deposit (see Fig. 3 and 4a,b).

The Au-Ag solid solutions are present of all stages of the formation of rodingites (see table 1), which is in good agreement with the model data showing the probability of their formation as a result of fluid discharge with the temperature 450°C and lower at gold variations from 0.1 to 10 ppm (Fig. 6b,d,f). The ratios of components of model Au-Ag solid solutions vary widely and depend on its deposition temperature and gold content in the solution. In natural samples, the composition of Au-Ag solid solutions, typically containing mercury as well, also vary widely, from kustelite and electrum in association with auricupride and tetra-auricupride of the first and second stages to high-fineness gold (Au>>Ag) among minerals of the third stage. Spiridonov and Pletnev (2002) reported that high-fineness gold is also common in chloritic rocks, chloritized and carbonatized serpentinites from the Karabash massif.

Metasomatic model for the formation of gold-bearing rodingites. In the metasomatic model the best correlation of natural mineral associations with the calculated ones is observed for the high-temperature fluid 350 and 450°C and W/R 10-100 (see Fig. 10), which characterizes the P-T-conditions of formation of the first and second stage rodingites. Under the influence of this fluid on rodingite, under rock-dominant regime (W/R<1), the initial three-mineral (chlorite+garnet+pyroxene) composition of rock becomes stable. When the degree of fluid-rock

499 interaction increases, the three-mineral association of the rodingite is replaced, at first, by two-
500 mineral (pyroxene+chlorite), and then by monomineral (chlorite) association (chloritite). At the
501 Karabash massif, pyroxene-chlorite rocks are rather widespread, especially in the southern part
502 of the rodingite belt, with the chlorites accompanying rodingites throughout the massif.

503 The model shows that interaction of low-temperature fluid with rodingite (250°C) results
504 in the occurrence, in addition to the main rodingite minerals, of a small amount of carbonate and,
505 finally, (at W/R > 10), quartz-chlorite rock with minor tremolite and talc. Carbonate (calcite), as
506 it was shown above, is typical of the third stage rodingites from the Zolotaya Gora deposit.
507 Within the limits of the metasomatic model, those segregations of carbonate can be discussed,
508 which replace earlier formed silicate minerals. Chlorite rocks with high contents of quartz in
509 natural rocks have not been found.

510 The metasomatic model includes most of accessory ore minerals which are typical of
511 gold-bearing rodingites: magnetite and sulfides of copper (chalcocite, bornite, chalcopyrite), Au-
512 Cu intermetallics (AuCu, $AuCu_3$, Au_3Cu), Au-Cu, Au-Ag and Au-Ag-Hg solid solutions, and
513 native copper. The paragenesis of magnetite with troilite (450°C) and troilite with chalcopyrite
514 (250-350°C) calculated for W/R <1 are not usual for the Zolotaya Gora deposit. At the same
515 time, typical for rodingites of stages 1 and 2 paragenesis of magnetite, chalcocite and bornite (T
516 = 350-450°C, W/R> 10), as well as chalcocite, bornite and native copper in carbonate veins of
517 stage 3 are formed in the metasomatic model (T = 250°C).

518 Formation of AuCu was observed on the interaction of rodingite with the fluid at 350 and
519 450°C in a wide range of W/R ratios (Fig. 8a,c). These data explain the formation of tetra-
520 auricupride in rodingites of the early stages and the more common occurrence of this mineral in
521 the deposit.

522 According to the metasomatic model $AuCu_3$ intermetallic is formed in gold-rich ores
523 (about 100 ppm) in a narrow range of W/R ~ 100, and slightly wider at 350°C (Fig. 8c).

Formation of this intermetallic completes the process of rock-fluid interaction, which agrees with the natural observations of the rather rare occurrence of auricupride in the Zolotaya Gora deposit and its overgrowth on tetra-auricupride.

Formation of Au_3Cu in model calculations was detected during the interaction of rodingite with a low-temperature fluid (T = 250°C) and high W/R >10 (Fig. 8e), i.e. stability conditions of chloritite. The narrow temperature range of stability of Au_3Cu and its occurrence only in the peripheral zone of rodingite alteration can be responsible for both the rare occurrence of Au_3Cu mineral at the deposit and its development on earlier deposited Au-Cu intermetallics (Spiridonov and Pletnev, 2002). Within the scope of the metasomatic model, the mineral Au_3Cu must be referred to the products of the late third stage of rodingites formation.

The wide occurrence of Au-Cu solid solutions in rodingites from the Karabash model was not clearly supported by the metasomatic model. In the calculations, a solid solution with a similar composition to Au_2Cu_3 (Fig. 8b), was established, which at the level of ore concentrations appears at 450°C in a W/R of about 100 (Fig. 8b) and at 250-450°C with W/R ~ 0.1 (see Fig. 8b,d,f).

Spiridonov and Pletnev (2002), suggested that Au-Cu solid solutions and intermetallics formed by replacing native copper. Our calculations within the framework of the metasomatic model have shown the inconsistency of such a mechanism for the formation of Au-Cu intermetallics. Copper-rich gold solid solutions ($Cu_{0.8\text{-}1.0}Au_{0.2\text{-}0}$) formed at W/R < 0.1 become unstable upon further interaction of the fluid with rodingite (see Fig. 8b,d,f). The native copper is stable at 250°C (see Fig. 7f), which is consistent with its presence among the minerals of the late third stage in the rodingites of Zolotaya Gora deposit.

Copper- and mercury-bearing Au-Ag solid solutions typical of the first and second stage rodingites are realized in the metasomatic model at 450 and 350°C (Fig. 8b,d), respectively, in the whole range of W/R from 0.1 to ~ 50-60. In the model, as in natural rodingite, fineness of

549 Au-Ag solid solutions vary from ~ 350 to 800‰ (see Fig. 8b,d and Fig. 3). When rodingite
550 interacts with a lower-temperature fluid (Fig. 8f), gold-silver phases (with fineness ~ 750‰) and
551 with high content of mercury (to 10-15 mol.%) stay stable.

552 Formation of Au-Cu intermetallics only under low f_{O2} and f_{S2} conditions is consistent with
553 the presence of these mineral assemblages in altered abyssal peridotites. Sulfur fugacity (fS_2)
554 during deposition of $AuCu_3$, AuCu and Au_3Cu in the Zolotaya Gora deposit matches the
555 conditions of low and very low sulfidation state (Fig. 11). It is considerably lower than fS_2 at the
556 formation of Au-Ag alloys of deposits in listvenites from the ophiolite massifs of South Urals
557 (Belogub et al., 2017, Spiridonov and Pletnev, 2002.)

558

559 ***7.3. The problem of the genesis of rodingite***

560 As it was shown above, the problem of the genesis of Karabash gold-bearing rodingite is
561 debatable. Metasomatic (Berzon, 1983; Murzin et al., 2006; Sazonov, 1998; Spiridonov and
562 Pletnev, 2002) and hydrothermal hypotheses of their formation were suggested by Murzin et al.
563 (2013).

564 The hydrothermal model (Fig. 10) assumes synchronous deposition of gold together
565 with other rodingite minerals, and that rodingite bodies themselves are hydrothermal veins
566 accompanied by metasomatic alteration of the host serpentinites. Thermodynamic calculations of
567 substitution reaction of antigorite by clinochlorine in the presence of aluminum ions in a wide
568 range of pH and T = 200–500°C (Rakhov, 2005) show that recognition of this substitution in an
569 alkaline medium requires a rather high total activity, which can be achieved only by in flow of
570 fluids, which result in the formation of rodingite.

571 As a source we consider a low-carbon dioxide chloride deep fluid which provide all the
572 main components of rodingites. The gold-bearing reduced low CO_2-water-chloride deep-source
573 fluids could be generated by: 1) decompression and autometamorphism of abyssal ultramafic

material by the ascending crustal-mantle fluids during the development of the Karabash massif (Kissin et al., 2016); or 2) dehydration of oceanic serpentinites (Murzin, 2006; Murzin et al., 2013). The source of water, gold and other components (Ca, Al, Ti, Cu, Ni, REE, P, etc.) in the fluid could be linked to metamorphic and metasomatic processes on the mafic-ultramafic rocks, with the discharging of fluids controlled by the high permeability of these rocks.

Hydrothermal model calculations show that Au-Cu intermetallics precipitate if the gold content in solution is no less than 0.5 ppm (see Fig. 6a,c,e). The study of gold solubility in metamorphic fluids with low salinity (Rauchenstein-Martinek et al., 2014) showed that a maximum gold-saturated solution may occur under the conditions of elevated gold content in metamorphosed parent rocks.

In the rodingites of the Karabash massif no relicts of any protolith rocks, except xenoliths of chloritized serpentinites, have been found. The presence of chrome-spinels in the rodingites suggests a connection with serpentinites (Berzon, 1983; Murzin et al., 2006; Sazonov, 1998), which are known to develop after ultramafic rocks (e.g. Evans et al., 2013). It was also established that the chemical composition of chrome-spinel from rodingites has the similar composition as chrome-spinel from the hosted serpentinites, developed after harzburgite and dunite.

Spiridonov and Pletnev (2002) considered dykes of Ti-rich gabbro and pyroxenites as protolihic rocks, which transformed into rodingite as a result of pre-ore regional metamorphism of the whole ultramafic massif. These authors suppose that chrome-spinel is present in rodingite as a xenolith captured by the melt during the intrusion of dikes. According to Spiridonov and Pletnev, (2002), gold minerals are deposited as a result of late listvenitization. But the typical listvenite minerals assemblage (quartz, sericite, calcite, dolomite) in the Zolotaya Gora deposit were not found by the present authors. Thus, for both models (metasomatic and hydrothermal)

598 we used reduced low CO_2-water-chloride fluid, but not CO_2-rich fluid which is common for the
599 formation of listvenites.

600 The thermodynamic modeling of the equilibria of rodingite minerals and gold minerals
601 agrees well with the observed gold-bearing paragenesis at the Zolotaya Gora deposit, both in the
602 hydrothermal and metasomatic models. The metasomatic model is better because it coincides
603 with mineral composition and mineral paragenesis in the Cu-Au-Ag-Hg system. In this model,
604 when the low-carbonate gold-bearing solution interacted with rodingite, the main rodingite
605 minerals remain stable both in the rock-dominating mode (W/R < 1) and in the fluid- dominating
606 mode (W/R > 1). In last case, as the W/R increases, the chlorite-garnet-pyroxene composition of
607 rodingite is replaced by the chloritite.

608 The logical consequence of the performed modeling can be the possibility of detection of
609 copper and gold in rodingites of both hydrothermal and metasomatic origin. Experimental and
610 theoretical modeling of gold mass transfer under conditions of bi-metasomatic rodingite
611 formation showed a rather limited concentration of gold, which takes place only locally within
612 the limits of the interaction zones of adjacent rocks (Molchanov et al., 2006; Plyusnina et al.,
613 2007). High concentrations of gold occur in the case of its additional introduction by the fluid. In
614 the hydrothermal model the rodingites in tectonically weak zones the level of mineralization can
615 be significant and controlled by gold content in a fluid and the availability of open spaces for
616 fluid flow. In the metasomatic model the validity for an economically viable gold content is
617 reached at a high W/R ~ 10.

618

619 **8. Conclusions**

620 1. The performed modeling for the formation of gold-bearing rodingites in the Zolotaya
621 Gora deposit indicates the possibility of equilibrium relationships of minerals of the system Cu-

Au-Ag-Hg with the rock-forming minerals of rodingites and consequently the ability of recognizing gold-bearing rodingites as a special type of gold mineral system.

The most complete correspondence of mineral composition and mineral paragenesis in the system Cu-Au-Ag-Hg is provided by the metasomatic model. In this model, early formed rodingite is considered as protolithic rock. When the gold-bearing low-carbon dioxide fluid interacts with the protolith the main minerals of rodingite remain stable in the rock-dominating mode (W/R <1). As W/R increases the chlorite-garnet-pyroxene composition of rodingite is replaced by a rock with predominance of chlorite. The metasomatic model predicts formation of all the gold minerals, which are known to occur in the Zolotaya Gora deposit, namely: Au-Cu, silver-bearing Au-Cu and copper-bearing Au-Ag solid solutions, as well as such intermetallics as auricupride($AuCu_3$), tetra-auricupride (AuCu) and Au_3Cu. Also in general paragenesis of gold minerals, chalcocite is present and it predominates over bornite and chalcopyrite.

2. In the metasomatic model Au-Cu intermetallics and Au-Ag solid solutions are formed throughout the temperature range 250-450°C. Au-Cu solid solution forms at temperature 250-450°C (W/R < 1) or 450°C (W/R > 10). Au-Ag-Hg solid solutions and native copper form at 250ºC only. The mechanism of replacement of native copper by gold-bearing phases, suggested by Spiridonov and Pletnev, (2002) in the metasomatic model was not confirmed by the calculations. In the hydrothermal model native copper and $AuCu_3$ were absent among of mineral phases, but other Au-Cu intermetallics (AuCu, Au_3Cu) precipitate if the gold content in solution is higher than 0.5 ppm.

3. Gold mineralization in rodingites may precipitate from gold-bearing water-chloride deeply-sourced fluid, with a low concentration of CO_2. At T < 350ºC, the main forms of gold in solution are sulfide complexes $Au(HS)_2^-$ and $AuHS^0$, while at higher temperature it occurs as $AuOH^0$.

4. Formation of Au-Cu intermetallics in the Zolotaya Gora deposit occurred under the effect of weak-acid hydrothermal solutions (pH = 3.5÷5) with low fugacity of O_2 and S_2: log f_{O2} = -26 ÷ -47, log f_{S2} = -8 ÷ -20.

Acknowledgments

This work was supported by the Russian Foundation for Basic Research (grant 16-05-00407a) and state assignment project (No.0330-2016-0001). We thank Reviewers for the very detailed reviews, many constructive comments, valuable suggestions and polishing of English.

References

Akinfiev, N.N., Zotov, A.V., 2001. Thermodynamic description of chloride, hydrosulfide, and hydroxo complexes of Ag(I), Cu(I), and Au(I) at temperatures of 25-500°C and pressures of 1-2000 bars. Geochemistry International 39,990-1006.

Akinfiev, N.N., Zotov, A.V., 2010. Thermodynamic description of aqueous species in the system Cu-Ag-Au-S-O-H at temperatures of 0-600°C and pressures of 1-3000 bar. Geochemistry International 48 (7), 714-720.

Amiour, L., Mermoul, S., Hamana, D., 2014. Study of the influence of silver addition on the orderdisorder transformations in Cu-Au system. Physics Procedia 55, 30-34.

Bach, W., Klein, F., 2009. The petrology of seafloor rodingites: Insights from geochemical reaction path modeling. Lithos 12 (1-2), 103-117.

Belogub E., Novoselov K., Melekestseva I., Zabotina M., Tret'yakov G., Zaykov V., Yuminov A., 2017. Listvenite-related gold deposits of the South Urals (Russia): a review. Ore Geol. Rev. 85, 247–270).

Berzon, R.O., 1983. Gold resource potential of ultramafics, VIEMS, Moscow (in Russian).

Bessinger, B., Apps, J.A., 2003. The hydrothermal chemistry of gold, arsenic, antimony, mercury and silver. http://repositories.cdlib.org/lbnl/LBNL-57395.

Breedveld, G.J.F., Prausnitz, J.M., 1973. Thermodynamic properties of supercritical fluids and their mixtures at very high pressure. AIChE Journal 19, 783-796.

Carmichael, I. S. E., Turner, F. J., Verhoogen, J. 1974. Igneous petrology. McGraw-Hili, New York, 739 pp

Chudnenko, K., Pal'yanova, G., 2013a. Thermodynamic properties of Ag-Au-Hg solid solutions. Thermochimica Acta 572, 65-70.

Chudnenko, K., Pal'yanova, G., 2013b. Thermodynamic properties of Au–Hg binary solid solution. Thermochimica Acta 566, 175-180.

Chudnenko, K.V., 2010. Thermodynamic Modeling in Geochemistry: Theory, Algorithms, Software, Applications. Academic Publishing House Geo, Novosibirsk (in Russian).

Chudnenko, K.V., Pal'yanova, G.A., 2014. Thermodynamic properties of solid solutions in the Ag-Au-Cu system. Russian Geology and Geophysics 55 (3), 349-360.

Chudnenko, K.V., Palyanova, G.A., 2016. Thermodynamic modeling of native formation Cu-Ag-Au-Hg solid solutions. Applied Geochemistry 66, 88-100.

686 Chudnenko, K.V., Pal'yanova, G.A., Anisimova, G.S., Moskvitin S.G., 2015. Ag-Au-Hg solid
687 solutions and physicochemical models of their formation in nature (Kyuchyus deposit as an
688 example). Applied Geochemistry 55, 138-151.
689 Coleman, R.G., 1977. Ophiolites. Springer Verlag., New York.
690 Damdinov, B.B., Zhmodik, S.M., Mironov, A.G., Ochirov, Yu.Ch., 2004. Noble-metal
691 mineralization in rodingite of the southeastern part of the Eastern Sayan. Geology and
692 Geophysics 45 (5), 577–587.
693 Diakonov, I., Pokrovski, G., Schott, J., Castet, S., Gout, R., 1996. An experimental and
694 computational study of sodium-aluminum complexing in crustal fluids. Geochimica et
695 Cosmochimica Acta 60, 197-211.
696 Dorogokupets, P.I., Karpov, I.K., 1984. Thermodynamics of minerals and mineral equilibria.
697 Novosibirsk, Nauka (in Russian).
698 Dubincka, E., Bylina, P., Kozlovski, A., Dorr, W., Nejbert, K., Schastok, J., Kulicki, C., 2004.
699 U-Pb dating of serpentinization: hydrothermal zircon from a metasomatic rodingite shell
700 (Sudetic ophiolite, SW Poland). Chemical Geology 203, 183-203.
701 Einaudi, M.T., Hedenquist, J.W., Inan, E.E., 2003. Sulfidation state of fluids in active and extinct
702 hydrothermal systems: transitions from porphyry to epithermal environments, in:
703 Simmons, S.F., Graham, I. (Eds.), Volcanic, geothermal and ore-forming fluids: Rulers and
704 witnesses of processes within the Earth. Society of Economic Geologists Special
705 Publication 10, pp. 285-314.
706 Escayola, M. P., Proenza, J. A., van Staal, C., Rogers, N. Skulski, T. 2009. The Point Rousse
707 listvenites, Baie Verte, Newfoundland: altered ultramafic rocks with potential for gold
708 mineralization? Newfoundland and Labrador Department of Natural Resources, Geological
709 Survey Report 09-1: 1-12
710 Evans, B. W., Hattori, K., Baronnet, A. 2013. Serpentinite: What, Why, Where? Elements 9, 99-
711 106
712 Galuskin, E., Zeleg, E., 2003. The first finding of Ag-amalgamates in rodingites (Naslawice,
713 Lower Silezia, Poland). Polskie Towarzystwo Mineralogisczne – Pracespecialne
714 mineralogical Society of Poland – Special papers Zeszyt. 22, 48-50.
715 Gunia, P., 1986. Rodingit z serpentinowokolic Mikolajowa (masyw serpentinitow y Braszowice-
716 Brzeznica, Dolny Slask). Geologia Sudetica 21(1), 197-229 (in Polish).

717 Helgeson, H.C., Delany, J.M., Nesbitt, H.W., Bird, D.K., 1978. Summary and critique of the
718 thermodynamic properties of rock-forming minerals. American Journal of Science 278A,
719 1-229.
720 Holland, T.J.B., Powell, R., 1998. An internally consistent thermodynamic data set for phases of
721 petrological interest. Journal of Metamorphic Geology 16 (3), 309-343.
722 Johnson, J.W., Oelkers, E.H., Helgeson, H.C., 1992. SUPCRT92: software package for
723 calculating the standard molal thermodynamic properties of mineral, gases, aqueous
724 species, and reactions from 1 to 5000 bars and 0 to 1000°C. Computers & Geosciences18,
725 899-947.
726 Karpov, I.K., Chudnenko, K.V., Kulik, D.A., 1997. Modeling chemical mass-transfer in
727 geochemical processes: thermodynamic relations, conditions of equilibria and numerical
728 algorithms. American Journal of Science 297, 767–806.
729 Kazachenko, V.T., Miroshnichenko, N.V., Perevoznikova, E.V., Karabtsov, A.A, 2008. Noble
730 metal minerals in metalliferous sediments of the triassic–jurassic carbonaceous sequence in
731 Sikhote Alin. Doklady Earth Sciences 421A, 919-922.
732 Kissin, A. Ju., Murzin, V.V., Pritchin, M.E., 2016. Tectonic position of the gold mineralization
733 of the Karabash Mountain (Southern Urals): Examination of mineralization of small
734 structural forms. Litosfera (4), 1-15. (in Russian)
735 Knight, J., Leitch, C.H.B., 2001. Phase relations in the system Au-Cu-Ag at low temperatures,
736 based on natural assemblages. Canadian Mineralogist 39, 889-905.
737 Kolonin, G.R., Paljanova G.A., Shironosova, G.P., Morgunov, K.G., 1994. Thermodynamic
738 model of potential gold-bearing high-temperature water-carbon-dioxide fluid.
739 Geochemistry International (12), 1725-1734.
740 Kolonin, G.R., Palyanova, G.A., Shironosova, G.P., Morgunov, K.G., 1997. The effect of
741 carbon-dioxide on internal equilibria in the fluid during the formation of hydrothermal gold
742 deposits. Geochemistry International (1), 46-57.
743 Koutsovitis P, Magganas A, Pomonis P, Ntaflos T., 2013. Subduction-related rodingites from
744 East Othris, Greece: mineral reactions and physicochemical conditions of formation.
745 Lithos 172–173, 139–157.
746 Kudryavtseva, A.I., Kudryavtsev, V.I., 2003. Occurrence of copper and silver gold in noble-
747 metal mineralization of the Southern Tuva ultrabasic rock belt. Conditions and
748 development of natural resources of Tuva and neighboring regions of Central Asia.
749 Geoecology of environment and society. Kyzyl: TuvIKOPR SB RAS. 45-48 (in Russian).

Laptev, Y.V., Pal'yanova, G.A., 2001. Experimental and thermodynamic study of silver solubility in water-chloride-carbon dioxide fluid. Geochemistry International 39 (2), 153-161.

Leblanc, M., Lbouabi, M., 1988. Native silver mineralization along rodingite tectonic contact between serpentinite and quartz diorite (Bou Azzer, Morocco). Economic Geology 83 (7), 1379-1391.

Lee, B.I., Kesler, M.G. 1975. Generalized thermodynamic correlation based on three-parameter corresponding states. AIChE Journal 21, 510-527.

Likhoidov, G.G., Plyusnina, L.P., 1992. Rodingites of northern Sakhalin and their physicochemical formation conditions. Tikhookeanskaya Geologya (2), 53–65 (in Russian).

Liu, Y., Wang, G., Wang, J., Chen, Y., Long, Z., 2012. Phase equilibria and thermodynamic functions for Ag–Hg and Cu–Hg binary systems. Thermochimica Acta 547, 83–88.

Lozhechkin, M.P., 1935. The Karabash deposit of cupriferous gold. Trudy UFAN SSSR (4), 35–44 (in Russian).

Mittwede, S.K., Schandl, E.S., 1992. Rodingites from the southern Appalachian Piedmont, South Carolina, USA. European Journal of Mineralogy 4(1), 7-16.

Molchanov, V.P., Plyusnina, L.P., Khanchuk, A.I., Zimin, S.S., Oktyabr'skii, R.A., 2006. Platinum- and gold-bearing rodingites of the Ust'-Dep ophiolite block (Middle Amur region). Doklady Earth Sciences 407 (2), 250-253.

Murzin, V.V., 2006. Origin of fluids responsible for the formation of Au-bearing rodingites based on isotope data: evidence from the Karabash Alpine-type ultramafic massif, the Southern Urals. Doklady Earth Sciences 407 (2), 254-257.

Murzin, V.V., Kudryavtsev, V.I., Berzon, R.O., Sustavov, S.G., 1987. Cupriferous gold in zones of rodingitization. Geology of Ore Deposits 29 (5), 96–99 (in Russian).

Murzin, V.V., Shanina, S.N., 2007. Fluid regime and origin of gold-bearing rodingites from the Karabash alpine-type ultrabasic massif, Southern Ural. Geochemistry International 45 (10), 998-1011.

Murzin, V.V., Sustavov, S.G., 1989. Solid-phase transformations in natural cupriferous gold. Izvestiya Akademii Nauk SSSR Seriya Geologicheskaya (11), 94-104 (in Russian).

Murzin, V.V., Varlamov, D.A., Ronkin, Yu.L., Shanina, S.N., 2013. Origin of Au-Bearing Rodingite in the Karabash Massif of Alpine-Type Ultramafic Rocks in the Southern Urals. Geology of Ore Deposits 55(4), 278-297.

783 Murzin, V.V., Varlamov, D.A., Shanina, S.N., 2006. Gold mineralization in rodingites of
784 Alpine-type ultrabasite massifs. Litosfera (1), 113–134.
785 Naumov, G.B., Ryzhenko, B.N., Khodakovsky, I.L, 1974. Handbook of Thermodynamic Data.
786 U.S. Geol. Surv.WRD-74-001 (in Russian).
787 Normand, C., Williams-Jones, A. E., 2007. Physicochemical conditions and timing of rodingite
788 formation: evidence from rodingite-hosted fluid inclusions in the JM Asbestos mine,
789 Asbestos, Québec. Geochemical Transactions 8 (11), 1-19.
790 Novgorodova, M.I., Tsepin, A.I., Kudrevich, I.M., Vyal'sov, L.N., 1977. New data on crystal
791 chemistry and properties of natural intermetallic compounds in the copper-gold
792 system. Zapiski Vsesojuznogo Mineralogicheskogo Obschestva106 (5), 540–552 (in
793 Russian).
794 Oen, I.S., Kieft, C., 1974. Nickeline with pyrrhotite and cubanite exsolutions, Ni-Co rich
795 loellingite and an Au-Cu alloy in Cr-Ni ores from Beni-Bousera, Morocco. Neues Jahrbuch
796 für Mineralogie / Monatshefte1, 1-8.
797 O'Hanley, D.S., Schandl, E.S., Wicks, F.J., 1992. The origin of rodingites from Cassiar British
798 Columbia, and their use to estimate T and P(H_2O) during serpentinization. Geochimica et
799 Cosmochimica Acta 56, 97-108.
800 Palandri, J.L., Reed, M.H., 2004. Geochemical models of metasomatism in ultramafic systems:
801 Serpentinization, rodingitization, and sea floor carbonate chimney precipitation.
802 Geochimica et Cosmochimica Acta 68, 1115-1133.
803 Pal'yanova, G.A., 2008. Physicochemical modeling of the coupled behavior of gold and silver in
804 hydrothermal processes: Gold fineness, Au/Ag ratios and their possible implications.
805 Chemical Geology 255, 399-413.
806 Perelyaev, A.P., 1948. Zolotaya Gora deposit, in: Ivanov, A.A., Rozkov, I.S. (Eds.), 200 years
807 of gold industry in the Urals, Ural Branch of SSSR Academy of Science, Sverdlovsk, pp.
808 285–295 (in Russian).
809 Plyusnina, L.P., Likhoidov, G.G., Molchanov, V.P., Shcheka, Zh.A., 2007. Modeling of gold
810 mass transfer during the listvanitization and rodingitization using the example of the Ust-
811 Dep ophiolite complex in the Upper Amur territory. Russian Journal of Pacific Geology. 1
812 (5), 464-472.
813 Plyusnina, L.P., Likhoidov, G.G., Zaraisky, G.P., 1993. Physicochemical formation conditions
814 of rodingite from experimental data. Petrologiya, 1 (5), 557–568.
815 Pirajno, F. 1992. Hydrothermal Mineral Deposits, Springer, Heidelberg, 709 pp

816 Pokrovski, G.S., Akinfiev, N.N., Borisova, A.Y., Zotov, A.V., Kouzmanov, K., 2014. Gold
817 speciation and transport in geological fluids: insights from experiments and physical-
818 chemical modelling. In book gold-transporting hydrothermal fluids in the earth's crust.
819 Geological Society Special Publications 402, London, 9-70.
820 Pokrovskii, V.A., Helgeson, H.C., 1995. Thermodynamic properties of aqueous species and the
821 solubilities of minerals at high pressures and temperatures: the system Al_2O_3-H_2O-NaCl.
822 American Journal of Science 295, 1255-1342.
823 Pokrovsky, P.V., Murzin, V.V., Berzon, R.O., Yunikov, B.A., 1979. Mineralogy of native gold
824 at the Zolotaya Gora deposit. Zapiski Vsesojuznogo Mineralogicheskogo Obshestva. 108
825 (3), 317–326(in Russian).
826 Puchkov V.N. Geology of the Urals and Cis-Urals (actual problems of stratigraphy, tectonics,
827 geodinamics and metallogeny). Ufa: DesignPoligraphService, 2010. 280p. (in Russian).
828 Puchkov V.N., 2017. General features relating to the occurrence of mineral deposits in the
829 Urals: What, where, when and why. Ore Geology Reviews. 85, 4–29.
830 Rakhov, E.V., 2005. Behavior of aluminum in chloritization zones in ultramafic rocks,
831 in Yearbook-2004, Yekaterinburg: Inst. Geol. Geochem., Ural Branch, Russian Academy
832 of Science, 206–211 (in Russian).
833 Rauchenstein-Martinek, K., Wagner, T., Wälle, M., Heinrich, C.A., 2014. Gold concentrations in
834 metamorphic fluids: A LA-ICPMS study of fluid inclusions from the Alpine orogenic belt.
835 Chemical Geology 385, 70–83.
836 Rechkin, A.N., 1974. A new type of gold mineralization in ultramafic rocks. Geology and
837 Geophysics 15 (2), 49–53.
838 Reid, R.C., Prausnitz, J.M., Sherwood, T.K., 1977. The properties of gases and liquids. McGraw-
839 Hill Book Company, New York.
840 Robie, R.A., Hemingway, B.S., 1995. Thermodynamic properties of minerals and related
841 substances at 298.15 K and 1 bar (10^5Pascals) pressure and at higher temperatures. U.S.
842 Geol. Survey Bull. 2131, United States government printing office, Washington.
843 Sazonov, V.N., 1998. Gold-productive metasomatic rocks in mobile belts: geodynamic settings
844 and PTX parameters of their formation and implications for forecasting. UGGGA.
845 Yekaterinburg (in Russian).
846 Schandl, E.S., Mittwede, S.K., 2001. Evolution of acipayam (Denizli, Turkey) rodingites.
847 International Geology Review 43 (7), 611-623.

Shandl, E.S., O'Hanley, D.S., Wicks, F.J., 1990. Fluid inclusions in rodingite: a geothermometer for serpentinization. Economic geology 85, 1273-1276.

Shock, E.L., Helgeson, H.C., Sverjensky, D.A., 1989. Calculation of the thermodynamic and transport properties of aqueous species at high pressures and temperatures: Standard partial molal properties of inorganic neutral species. Geochimica et Cosmochimica Acta 53, 2157-2183.

Shock, E.L., Sassani, D.C., Willis, M., Sverjensky, D.A., 1997. Inorganic species in geologic fluids: Correlation among standard molal thermodynamic properties of aqueous ions and hydroxide complexes. Geochimica et Cosmochimica Acta 61, 907–950.

Seravkin, I.B., Znamenskii, S.M., Kosarev, A.M., 2003. The Main Ural Fault in the South Urals: Structure and the Main Evolution Phases. Geotectonics (3), 42-64.

Snachyov, A.V., Kuznetsov, N.S., Snachyov, V.I., 2011. The Chernoe ozero gold occurrence in carbonaceous deposits of the ophiolite association: The first object of such a type in the Soutern Urals. Doklady Earth Sciences 439 (1), 906-908 (in Russian).

Spiridonov, E.M., Pletnev, P.A., 2002. Zolotaya Gora deposit of cupriferous gold, Moscow. Systems. Nauka, Moscow (in Russian).

Sverjensky, D.A., Shock, E.L., Helgeson H.C., 1997. Prediction of the thermodynamic properties of aqueous metal complexes to 1000°C and 5 kb. Geochimica et Cosmochimica Acta 61, 1359–1412.

Tagirov, B.R., Baranova, N.N., Zotov, A.V., Schott, J., Bannykh, L.N., 2006. Experimental determination of the stabilities of Au_2S(cr) at 25°C and $Au(HS)_2^-$ at 25-250°C, Geochimica et Cosmochimica Acta 70, 3689-3701.

Tanger, J.C., Helgeson, H.C. 1988.Calculation of the thermodynamic and transport properties of aqueous species at high pressures and temperatures: revised equations of state for standard partial molal properties of ions and electrolytes. American Journal of Science 288, 19–98.

Tsikouras, B., Karipi, S., Rigopoulos, I., Perraki, M., Pomonis, P., Hatzipanagiotou, K. 2009. Geochemical processes and petrogenetic evolution of rodingite dykes in the ophiolite complex of Othrys (Central Greece). Lithos 113(3-4), 540-554

Vallis, F., Scambelluri, M., 1996. Redistribution of high-pressure fluids during retrograde metamorphism of eclogite-facies rocks (Voltri Massif, Italian Western Alps). Lithos 39, 81-92.

Vol, A.E., Kagan, I.K., 1976. Structure and Properties of Binary Metal. Nauka, Moscow.

Walas, S.M., 1985. Phase equilibria in chemical engineering. Butterworth Publ., Boston.

Williams, G. J. 1974. Economic geology of New Zealand. The Australasian Institute of Mining and Metallurgy, Monograph No 4, 490 pp

Zhmodik, S.M., Mironov, A.G., Derevenets, V.G., et al., 1998. A new type of tin-(mercury)-gold-PGE ore mineralization in the Eastern Sayan Range, Doklady Earth Sciences 361 (6), 782–785.

Zhmodik, S.M., Mironov, A.G., Zhmodik, A.S., 2008. Gold-concentrating systems of ophiolite belts (by the example of the Sayan-Baikal-Muya belt). Academic publishing House Geo. Novosibirsk (in Russian).

Zoheir, B., Lehmann, B. 2011. Listevenite-lode association at the Barramiya gold mine, Eastern Desert, Egypt. Ore Geology Reviews 39, 101-115.

Figure captions

Figure 1.

A – Position of Zolotaya Gora gold-rodingite deposit within the tectonic setting of the Urals (modified after Puchkov, 2010).

B – Schematic geology map of the Karabash massif (modified after Snachyov et al., 2011) with authors' additions.

Figure 2. Tectonic contacts between the rodingite and chloritized serpentinite. The wall of the open pit in the southern part of the Zolotaya Gora deposit.

a. Laminated chlorite-garnet-diopside rodingite (1) in chloritized serpentinite (2).

b. Vein of late diopside rodingite (1) in antigorite serpentinite (2).

Figure 3. Composition of Au-Ag-Cu-Hg minerals of the Zolotaya Gora deposit (in wt.%).

Figure 4. Typical intergrowths of gold minerals in rodingites from Zolotaya Gora deposit. BSE images.

a. Thin exsolution of Ag, Hg-bearing gold-copper solid solution of composition ~$Au_3Cu_2Ag_{0.0n}Hg_{0.0n}$: tetra-auricupride AuCu (dark phase) and phase similar in composition to Au_2Cu (light phase) with minor admixtures of silver and mercury.

b. Lens-like segregations of Hg-bearing gold-silver phase (light phase) and plates of tetra-auricupride AuCu (dark phase) in solid solution Au_2Cu.

c. Tetra-auricupride AuCu (in wt.%: Au 75.0; Cu 21.8; Hg 0.1.) with ingrowths of Hg-bearing electrum (El) (in wt.%: Au 68.9; Ag 24.8; Cu 0.7; Hg 3.9). White spongy is high-fineness gold (in wt.%: Au 96.5; Ag 0.7; Cu 1.0; Hg 0.4).

d. $AuCu_3$ intergrown with diopside (Di), andradite (Ad) and chlorite (Chl). El - Mercury-bearing electrum (in wt.% - Au 41.1; Ag 54.7; Hg 4.3).

Figure 5. Species in aqueous solution and solid phases for Au (a, b), Ag (c, d) and Cu (e, f) in the hydrothermal model with 1 ppm Au and W/R =10.

Figure 6. Results of thermodynamic calculations of hydrothermal model: distribution of gold among solid phases (in wt.%) at specified Au content in fluid (a, c, e) and the composition of disordered solid solution Au-Ag-Cu(-Hg) (in mol.%) at the specified content of Au in fluid (b, d, f).

925

926 **Figure 7.** Model of water-rock interaction for different P,T-conditions a, c, e – mineral
927 composition of rodingite; b, d, f – variation trends of minor minerals, log f_{O2}, log f_{S2} and pH.

928

929 **Figure 8.** Model of water-rock interaction for different P-T-conditions.
930 a, c, e – amount of gold solid phases; b, d, f – distribution of components in disordered solid
931 solution Au-Ag-Cu-Hg.

932

933 **Figure 9.** Contents in wt% of carbonate, quartz and graphite in the metasomatic model for
934 rodingite formation as a function of W/R and degrees of CO_2 saturation of fluid (0.4, 4 and 40
935 mol. % CO_2) under 250ºC, 350 ºC и 450 ºC.

936

937 **Figure 10.** Scheme of rodingite formation according to calculations for hydrothermal and
938 metasomatic models.
939 Abbreviations: ss – solid solutions; Ore minerals: Bn – bornite, Cpy – chalcopyrite, Cc –
940 chalcocite, Mt – magnetite, Tro – troilite, Au_3Cu – mineral Au_3Cu, AuCu – tetra-auricupride,
941 $AuCu_3$ – auricupride, Cu – native copper. Minerals of rodingite: Px – pyroxene, Chl – chlorite,
942 Gar – garnet, Tr – tremolite, Tc – talc, Gr – graphite, Qz – quartz, Car – carbonate.

943

944 **Figure 11.** Sulfur fugacity versus temperature diagram (modified from Einaudi et al., 2003)
945 showing the formation conditions of Au-Cu intermetallics in rodingites from Zolotaya Gora
946 deposit and those of Au-Ag solid solutions in listvenites of South Urals.

947

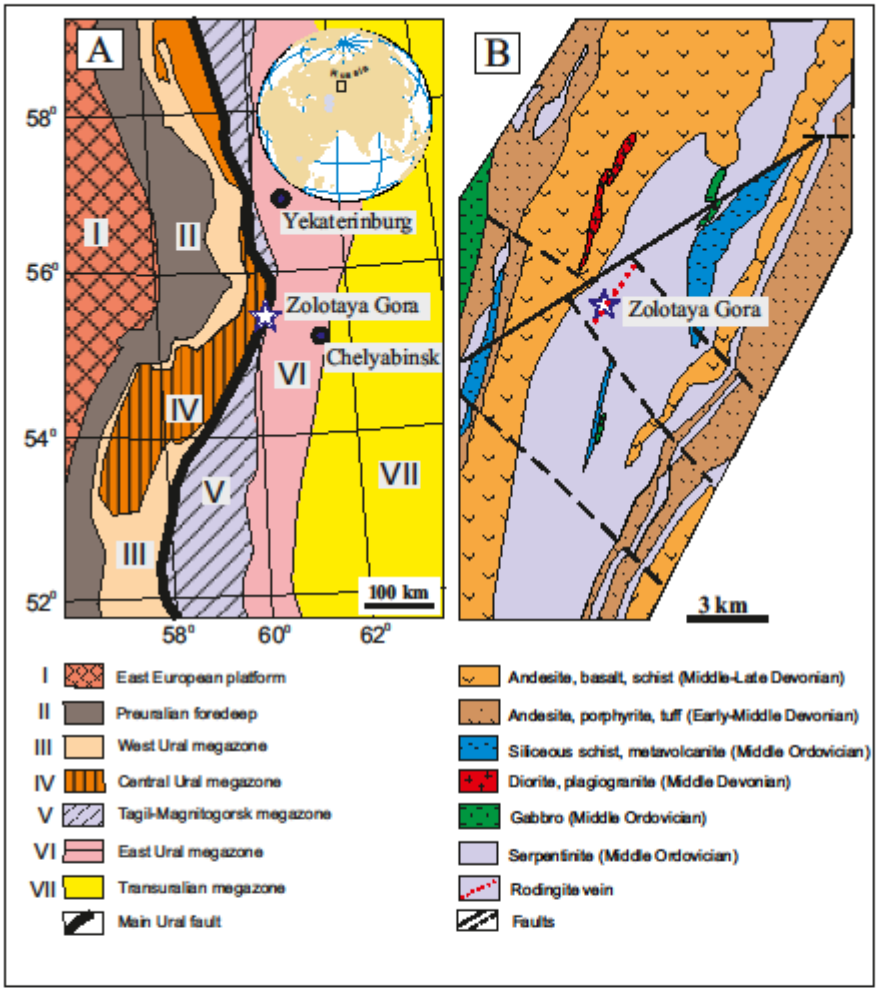

948

949

Fig.2

950

951

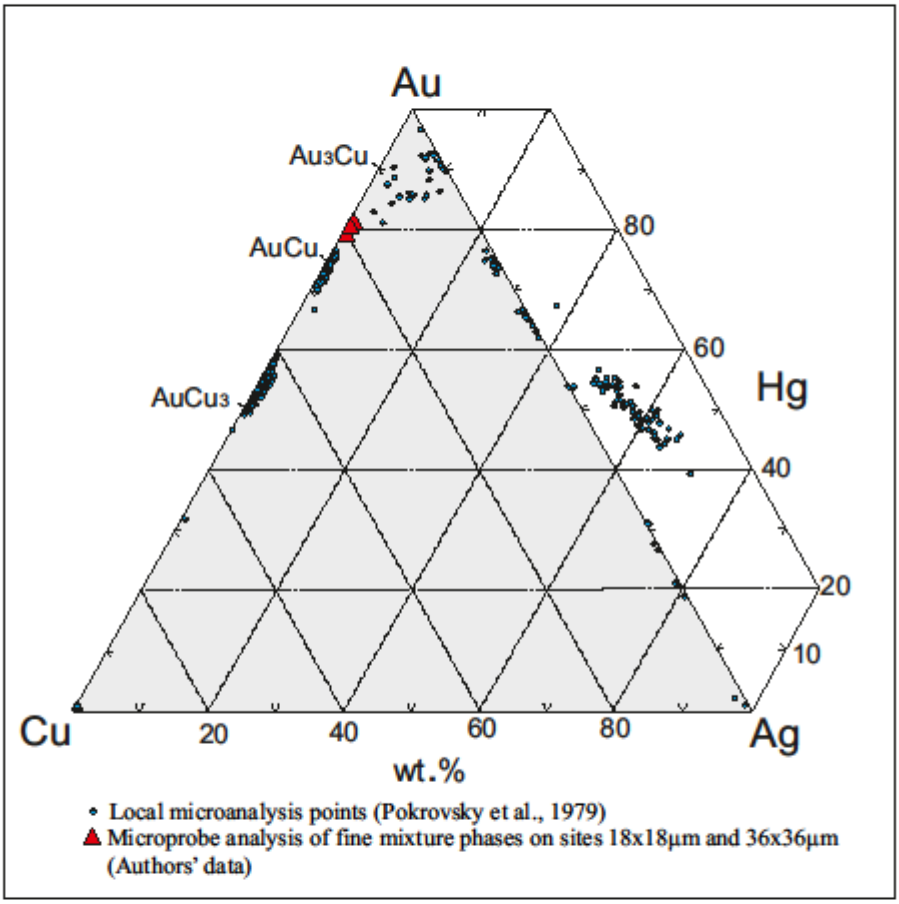

Fig.3

Fig.4

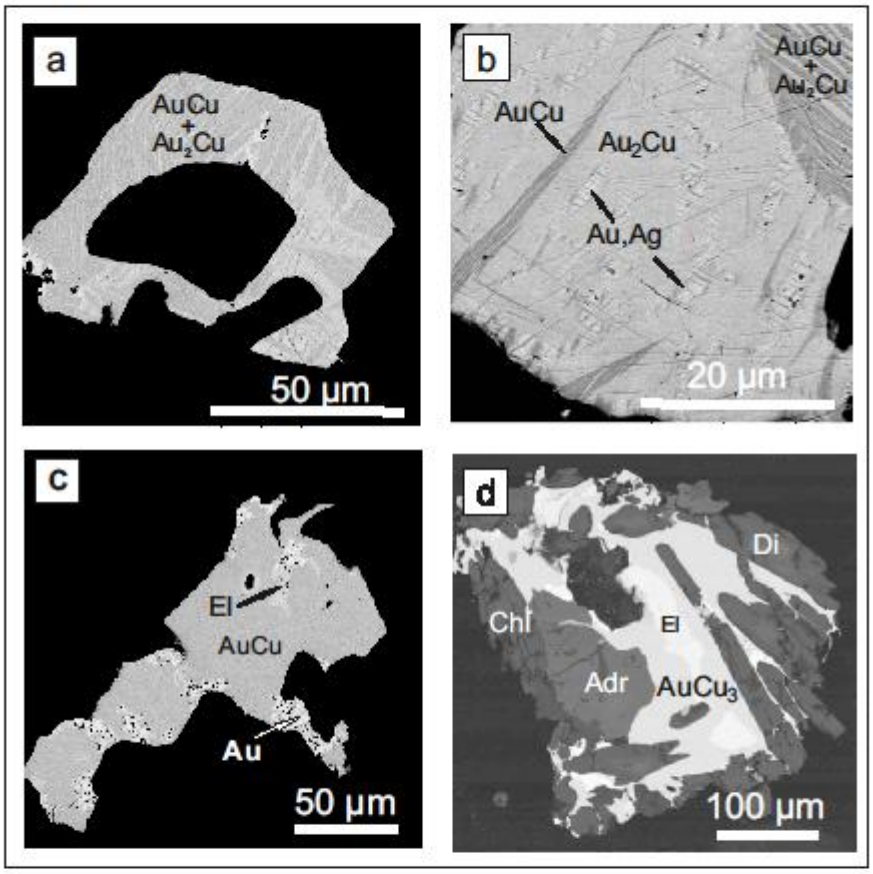

954

955

Fig. 5

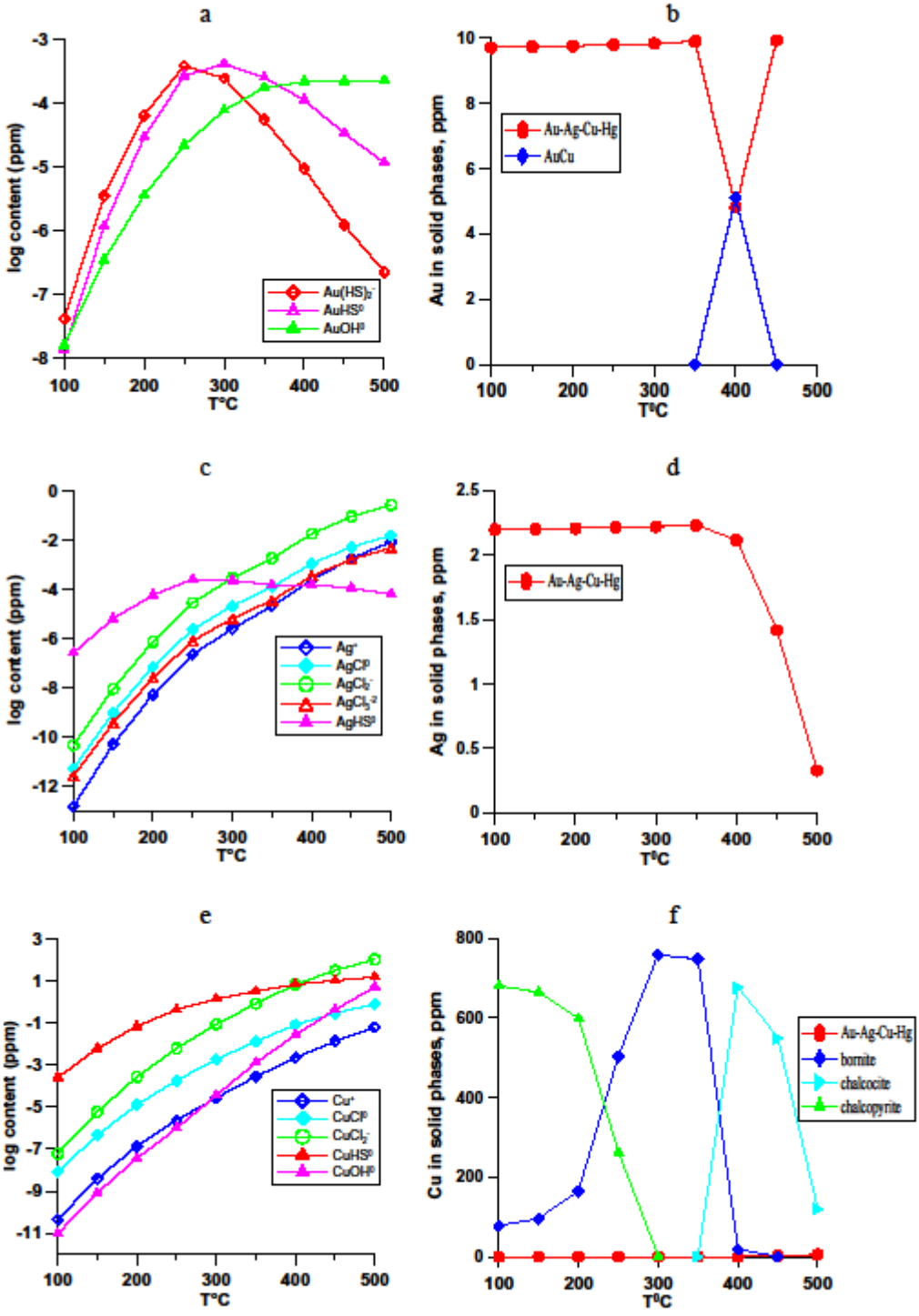

956

957

Fig. 6

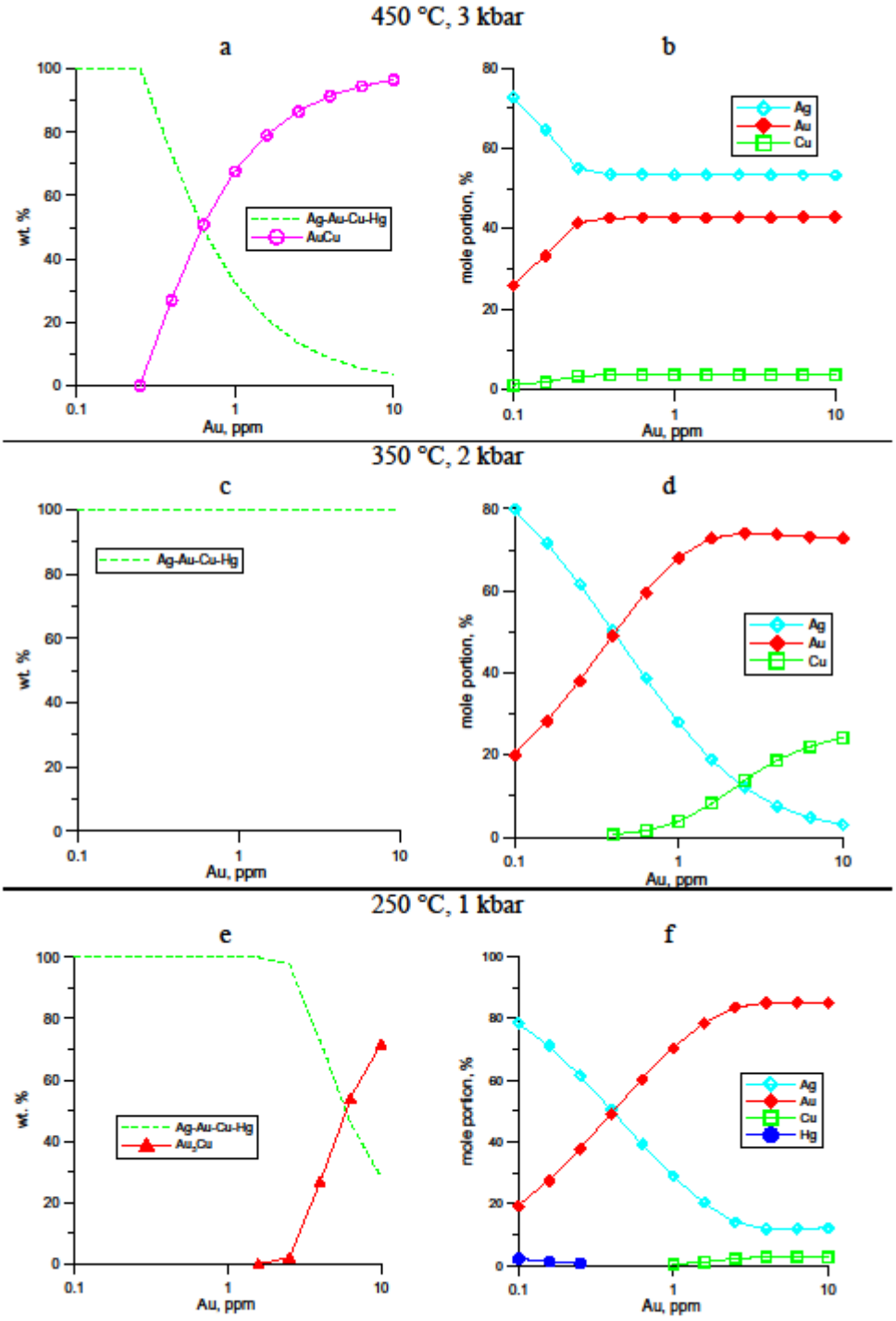

958

959

Fig. 7

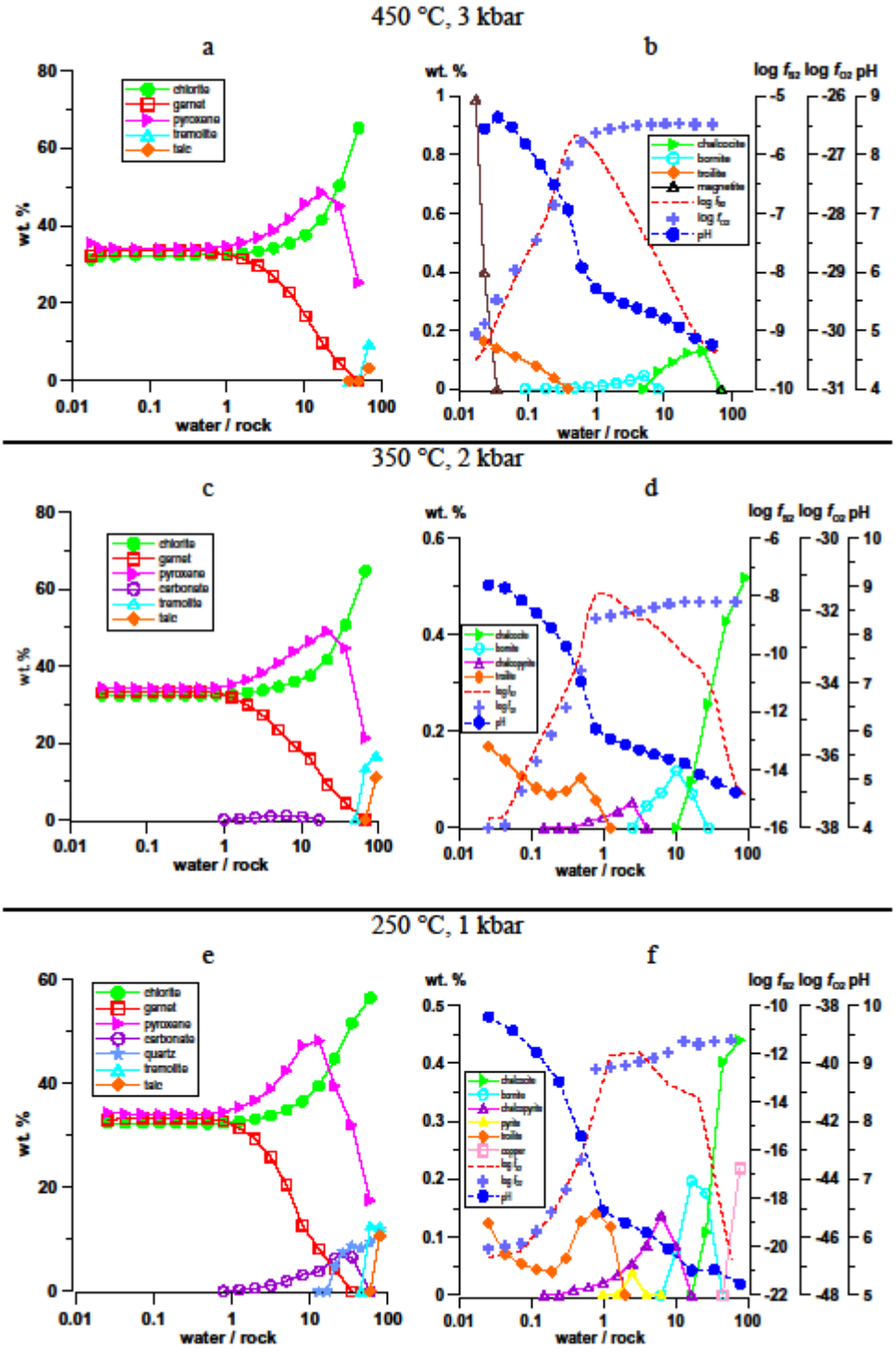

960

961

Fig. 8

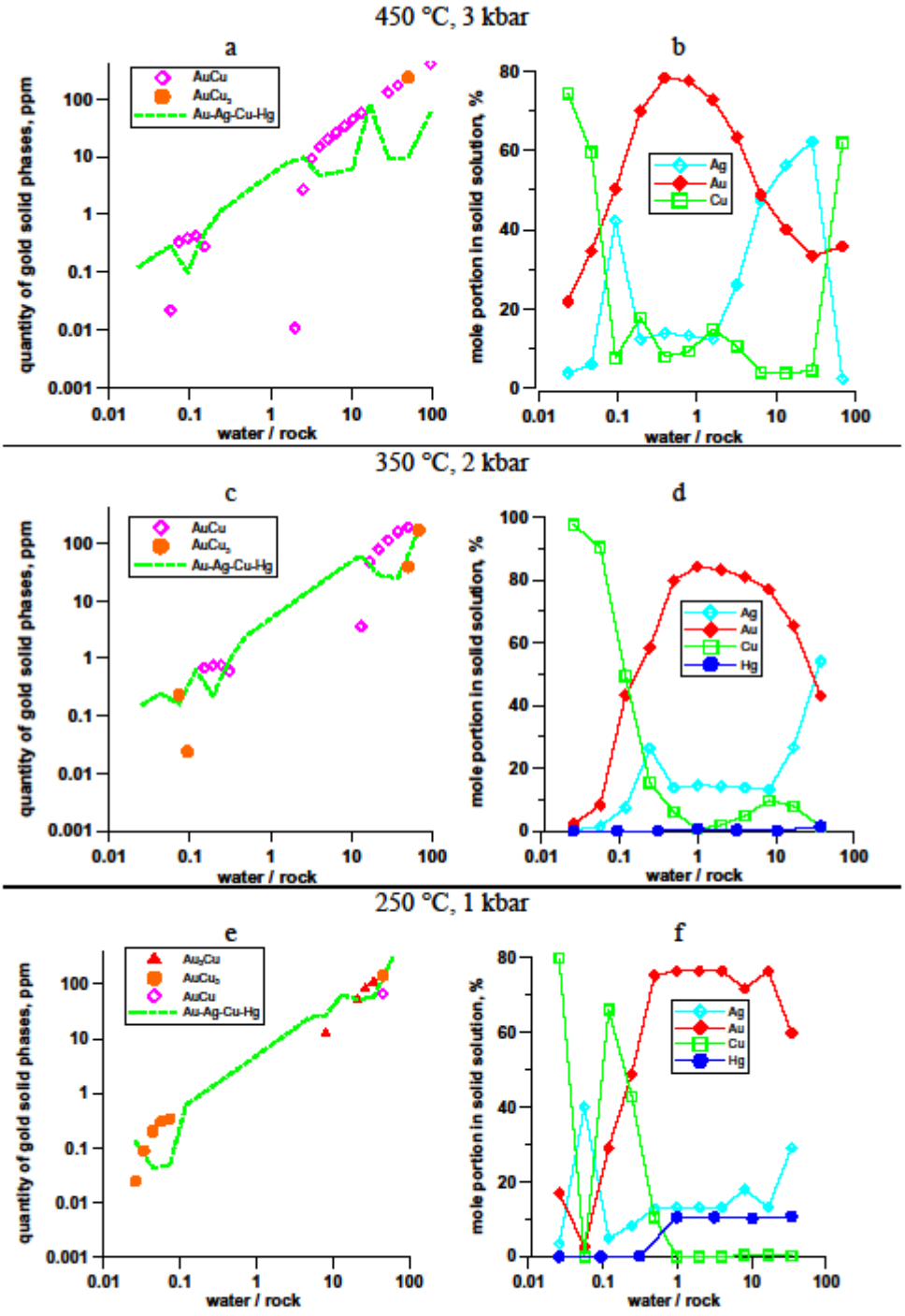

962

963

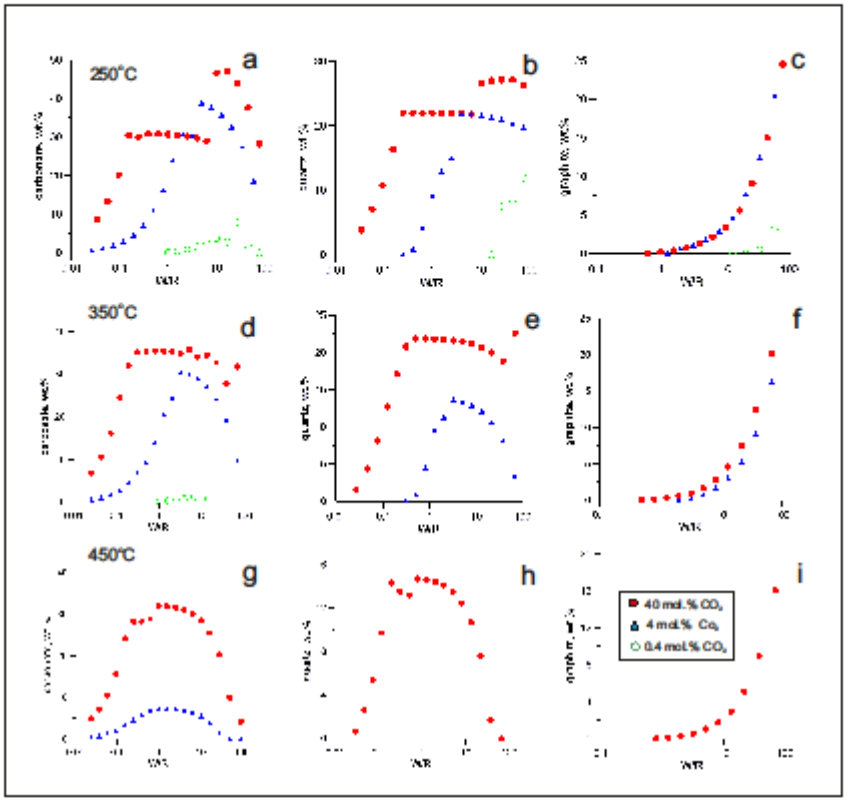

Fig.9

964

965

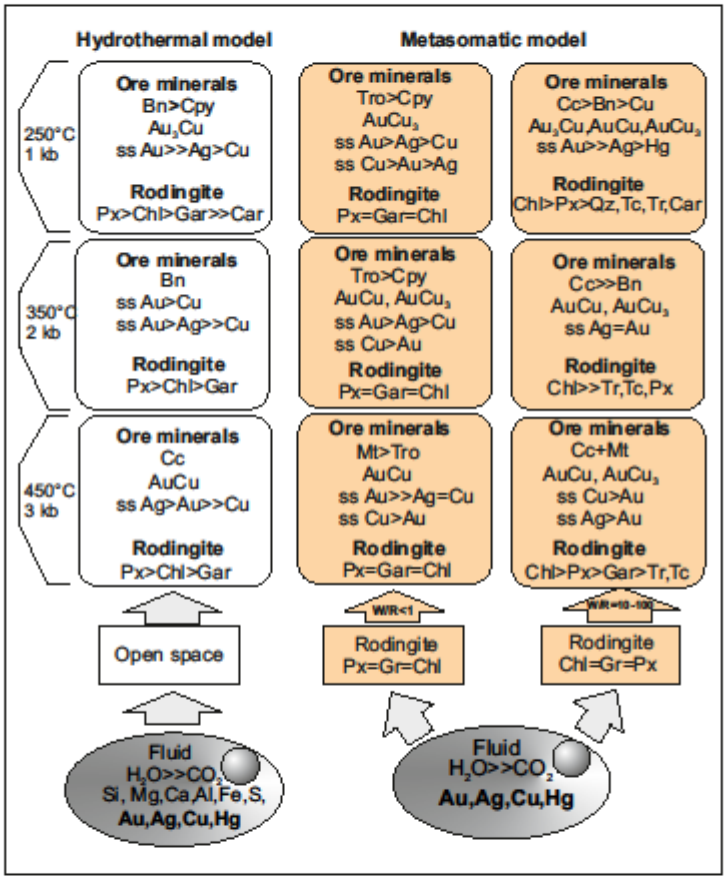

Fig.10

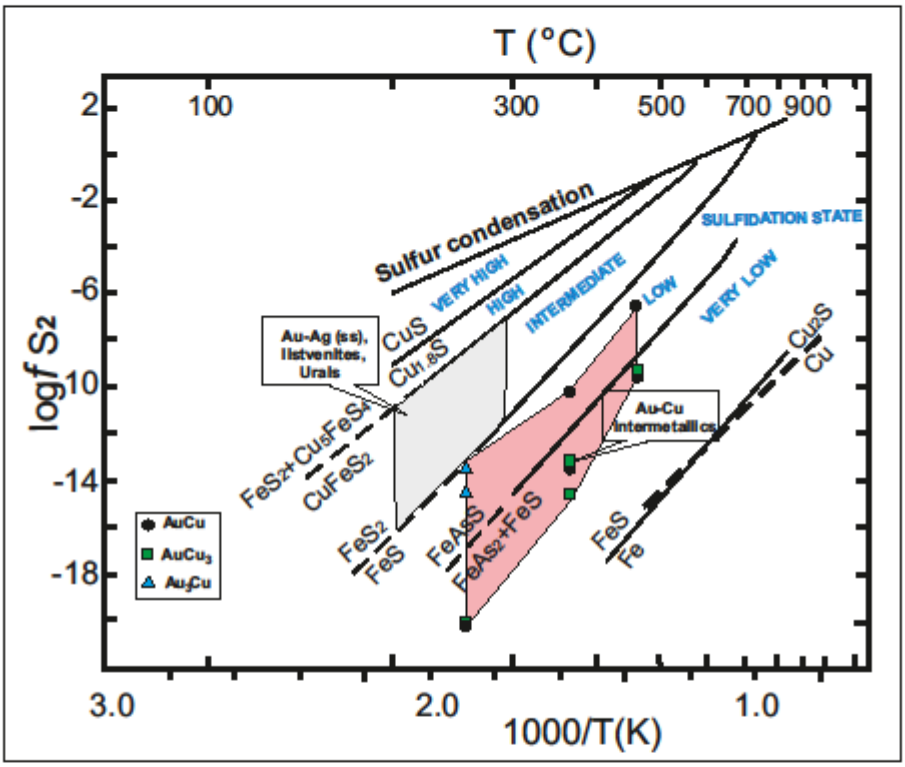

Fig.11

968

969

970 **Table 1.** Minerals of rodingites and chloritolites at Zolotaya Gora deposit (Spiridinov and Pletnev,
971 2002; Murzin et al., 2013).

Minerals	Stage mineralization		
	1	2	3
	Rodingites		
Main	Chlorite (clinochlore, pennine), garnet (Ti-hydroandradite), clinopyroxene (diopside)	Clinopyroxene (diopside), garnet (hydroandradite)	Calcite
Minor	Vesuvianite, apatite	Chlorite (pennine), apatite, magnetite, ilmenite, dolomite, calcite	Chlorite (pennine), magnetite
Accessory	Mn-Zn-chrome-spinellid, chalcocite, nickeline, maucherite, native copper, zircon, baddeleyite, thorianite, allanite -(Ce), uraninite	Titanite, perovskite, calcioancylite-(Ce), native copper, maucherite, chalcocite, chalcopyrite, bornite, Co-pentlandite, Co-cupropentlandite	Titanite, ilmenite, chalcocite, bornite, rutile, cuprite, galena, greenockite, native Cu, Sb and Pb, antimonides Cu, Ni, Fe (nisbite, seinäjokite, cuprostibite, zlatogorite, gudmundite, ullmannite, breithauptite)
Minerals of gold	Hg-Ag-containing gold-copper solid solutions, Hg-containing native gold	Tetra-auricupride, auricupride, Hg-containing native gold	Native gold, Hg-silver
	Chloritolites		
Main	Chlorite (clinochlore, pennine)	Chlorite	Chlorite
Secondary	Fe-diopside, antigorite, magnetite	Magnetite	Calcite
Accessory	Apatite, native copper, pentlandite, heazlewoodite	Chalcocite, pentlandite, maucherite, orcelite, nickeline, heazlewoodite, godlevskite, millerite	Magnetite
Minerals of gold		Solid solutions AuCu - Au_3Cu_2 - Au_3Cu	

972

973
974

975

976 **Table 2.** Components of aqueous solution and gases taking into account in thermodynamic models

977

aqueous solution							
component	ref.	component	ref.	component	ref.	component	ref.
$Ag(CO_3)^-$	1	$CaCl_2^0$	1	$MnCl^+$	5	HgO^0	5
$Ag(CO_3)_2^{-3}$	1	$CaHCO_3^+$	3	$MnSO_4^0$	5	$HgOH^+$	5
$Ag(OH)_2^-$	3	$CaHSiO_3^+$	1	Fe^{+2}	5	$HgS(HS)^-$	9
Ag^+	2	$CaOH^+$	5	Fe^{+3}	5	K^+	5
Ag^{+2}	2	$CaSO_4^0$	1	$FeCl^+$	1	KCl^0	1
$AgCl^0$	3	Cl^-	5	$FeCl^{+2}$	1	$KHSO_4^0$	1
$AgCl_2^-$	3	$Cu(HS)_2^-$	4	$FeCl_2^0$	1	KOH^0	5
$AgHS^0$	4	$Cu(OH)_2^-$	3	FeO^0	5	KSO_4^-	1
AgO^-	5	Cu^+	5	FeO^+	5	$CH4^0$	6
$AgOH^0$	3	Cu^{+2}	2	FeO_2^-	5	Mg^{+2}	5
$Al(OH)^{+2}$	6	$CuCl^0$	3	$FeOH^+$	5	$MgCO_3^0$	2
$Al(OH)_2^+$	7	$CuCl^+$	1	$FeOH^{+2}$	5	$MgCl^+$	1
$Al(OH)_3^0$	8	$CuCl_2^0$	1	HCO_3^-	5	$MgHSiO_3^+$	1
$Al(OH)_4^-$	8	$CuCl_2^-$	3	HCl^0	6	$MgOH^+$	5
Al^{+3}	6	$CuCl_3^-$	1	$HFeO_2^0$	5	$MgSO_4^0$	6
$Au(HS)_2^-$	4	$CuCl_4^{-2}$	1	$HFeO_2^-$	5	Na^+	5
$Au(OH)_2^-$	3	$CuHS^0$	3	$HHgO_2^-$	5	$NaCl^0$	1
Au^+	3	CuO^0	5	H_2S^0	9	$NaHSiO_3^0$	1
Au^{+3}	5	CuO_2^{-2}	5	HS^-	9	$NaOH^0$	5
$AuCl^0$	3	$CuOH^0$	3	HSO_4^-	5	$NaSO_4^-$	6
$AuCl_2^-$	3	$CuOH^+$	5	$Hg(HS)_2^0$	9	SO_4^{-2}	5
$AuHS^0$	4	Mn^{+2}	5	$Hg(OH)_2^0$	9	$HSiO_3$	1

$AuOH^0$	3	Mn^{+3}	5	Hg^0	9	SiO_2^0	6
CO^0	6	MnO_4^-	5	Hg^{+2}	2	H_2^0	2
CO_2^0	6	MnO_4^{-2}	5	Hg_2^{+2}	5	O_2^0	2
CO_3^{-2}	5	$MnOH^+$	5	$HgCl^+$	1		
Ca^{+2}	5	MnO^0	5	$HgCl_2^0$	1		
$CaCO_3^0$	1	$HMnO_2^-$	5	$HgCl_3^-$	1		
$CaCl^+$	1	MnO_2^{-2}	5	$HgCl_4^{-2}$	1		

gases

component	ref.	component	ref.	component	ref.	component	ref.
HCl	10	H_2S	10	CO_2	10	S_2	10
H_2	10	CO	10	CH_4	10	SO_2	10

978

979 1 - Sverjensky et al., 1997; 2 - Shock et al., 1989; 3 - Akinfiev and Zotov, 2001; 4 - Akinfiev and Zotov,
980 2010; 5 - Shock et al., 1997; 6 - Johnson et al., 1992; 7 - Pokrovskii and Helgeson, 1995; 8 - Diakonov et
981 al., 1996; 9 - Bessinger and Apps, 2003; 10 - Reid et al., 1977.

982

983

984 **Table 3.** Solid phases components used in thermodynamic models

985

986

mineral	formula	ref.	mineral	formula	ref.
Ag-Au-Cu-Hg	Au	1	Tenorite	CuO	3
	Ag	1	Diopside	$CaMg(SiO_3)_2$	3
	Cu	1	Montroydite	HgO	4
	Hg	1	Akermanite	$Ca_2MgSi_2O_7$	3
Au_3Cu	Au_3Cu	1	Albite	$NaAlSi3O_8$	2
Tetra-auricupride	AuCu	1	K-feldspar	$KAlSi3O_8$	2
Auricupride	$AuCu_3$	1	Tremolite	$Ca_2Mg_5Si_8O_{22}(OH)_2$	3
Chlorite	$Mg_6Si_4O_{10}(OH)_8$	2	Anhydrite	$CaSO_4$	3
	$Mg_4Al_4Si_2O_{10}(OH)_8$	2	Bornite	Cu_5FeS_4	3
	$Mg_5Al_2Si_3O_{10}(OH)_8$	2	Plagoiclase	$NaAlSi_3O_8$	2
	$Fe_5Al_2Si_3O_{10}(OH)_8$	2		$CaAl_2Si_2O_8$	2
Garnets	$Fe_3Al_2Si_3O_{12}$	2	Dolomite	$CaMg(CO_3)_2$	2
	$Ca_3Fe_2Si_3O_{12}$	2	Ferrosilite	$FeSiO_3$	3
	$Ca_3Al_2Si_3O_{12}$	2	Ferrous-oxide	FeO	3
	$Mg_3Al_2Si_3O_{12}$	2	Graphite	C	2
	$Mn_3Al_2Si_3O_{12}$	2	Halite	$NaCl$	3
Pyroxenes	$CaMgSi_2O_6$	2	Hematite	Fe_2O_3	2
	$CaFeSi_2O_6$	2	Huntite	$CaMg_3(CO_3)_4$	3
	$NaAlSi_2O_6$	2	Magnetite	Fe_3O_4	2
Carbonates	$CaCO_3$	2	Pyrite	FeS_2	3
	$MgCO_3$	2	Troilite	FeS	3
	$MnCO_3$	2	Quartz	SiO_2	2
	$FeCO_3$	2	Rutile	TiO_2	2

Chalcocite	Cu_2S	3	Sphene	$CaTiSiO_5$	2
Chalcopyrite	$CuFeS_2$	3	Mercury	Hg	3
Silver (I) oxide	Ag_2O	4	Sulfur	S	7
Chlorargyrite	AgCl	5	Talc	$Mg_3Si_4O_{10}(OH)_2$	2
Petrovskaite	AgAuS	6	Olivine	Fe_2SiO_4	2
Chrysotile	$Mg_3Si_2O_5(OH)_4$	3		Mg_2SiO_4	2
Cinnabar	α-HgS	3	Antigorite	$Mg_3Si_2O_5(OH)_4$	8
Metacinnabar	β-HgS	3	Crisotile	$Mg_3Si_2O_5(OH)_4$	2
Copper	Cu	3	Lisardite	$Mg_{5.5}AlSi_{3.5}O_{10}(OH)_8$	8
Covellite	CuS	3			
Cuprite	Cu_2O	3			

987

988 1 – Chudnenko and Pal'yanova, 2016; 2 – Holland and Powell, 1998; 3 – Helgeson et al., 1978; 4 – Naumov
989 et al., 1974; 5 – Robie and Hemingway, 1995; 6 – Tagirov et al., 2006; 7 – Shock et al., 1997; 8 –
990 Dorogokupets and Karpov, 1984.

991

992 **Table 4.** The chemical composition of chlorite-garnet-pyroxene rodingite (in wt.%) (Archival
993 materials Lozhechkin, 1935) and antigorite-serpentinite (Berzon, 1983) used in calculations
994
995

Components	Serpentinite	Rodingite
SiO_2	40.47	41.78
TiO_2	0.04	bdl
Al_2O_3	1.44	8.32
FeO	1.61	3.95
Fe_2O_3	5.31	5.32
CaO	0.48	20.27
MnO	0.09	0.45
MgO	38.21	16.6
Na_2O	0.12	0.20
K_2O	0.03	bdl
H_2O	10.59	3.38
CO_2	0.46	bdl
SO_3	0.75	0.07

996 bdl - below detection limit

997
998

999 **Table 5.** Composition and characteristics of model hydrothermal solution

1000

Components	mol/kg (H_2O)
C	2.300e-01
Cl	1.100e-01
Cu	1.202e-03
Ag	4.348e-06
Au	5.077e-06
Hg	3.391e-05
H	1.683e+00
O	4.564e-01
T, °C	650
P, kbar	4
pH	1.97

1001

1002

1003 **Table 6.** Conditions of the formation of Au-Cu intermetallics

1004

Intermetallic	Temperature, °C	log f_{S2}	log f_{O2}	pH
AuCu	450	-6.5 ÷ -9.4	-26.5 ÷ -30.5	4.5 ÷ 8.3
	350	-10.1 ÷ -13.3	-32 ÷ -37	4.9 ÷ 8.3
	250	-20.3	-47	5.4
$AuCu_3$	450	-9.4	-30	4.8
	350	-13.3 ÷ -14.5	-31.5 ÷ -37	4.7-8.7
	250	-20.2 ÷ -20.4	-38.5 ÷ -47	5.4 ÷ 9.8
Au_3Cu	450	-	-	-
	350	-	-	-
	250	-13.3 ÷ -14.5	-46 ÷ -47	5.4 ÷ 5.8

1005

1006

1007 Highlights

1008 • Cu-Ag-Au-Hg mineralization in rodingites of the Zolotaya Gora Au deposit
1009 is described
1010 • Au-Cu solid solution and intermetallics (Au_3Cu, AuCu, Au_3Cu) were
1011 formed at T >250°C
1012 • Native gold with impurity of Hg and Cu was formed at T <300°C.

1013

1014